



Photoemission from Biased Metal Surfaces

Quantum efficiency, Laser heating, Dielectric Coatings, and
Quantum Pathways Interference

Yang Zhou

Department of Electrical and Computer Engineering

Michigan State University

zhouya22@msu.edu

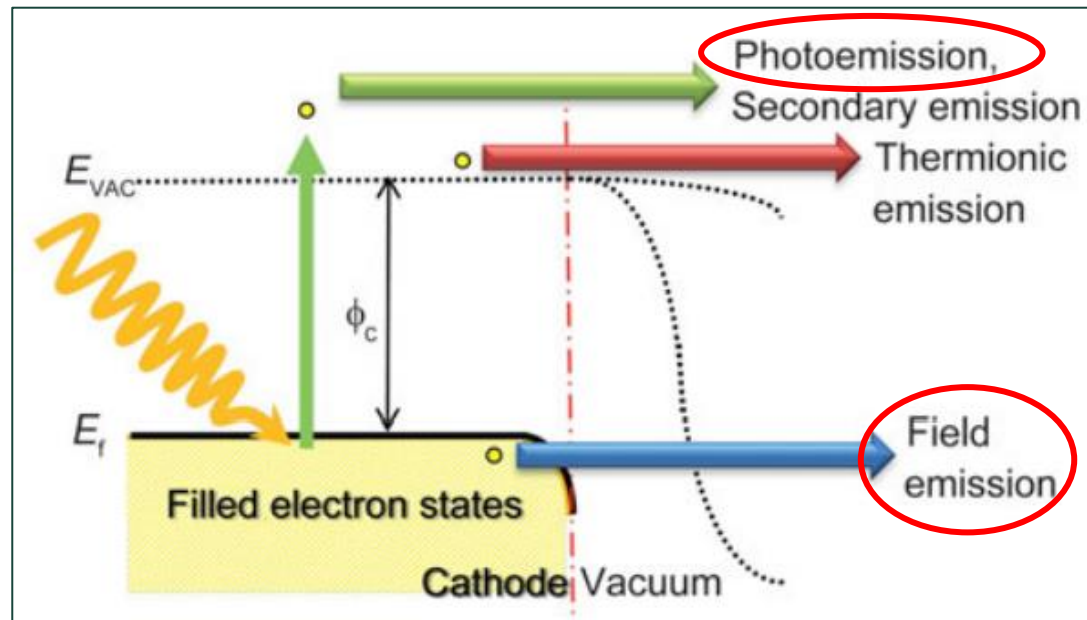
March 2, 2023

Outline

- **Background & Motivation**
- **Research Overview**
- **Effects of laser wavelength & heating**
- **Effects of cathode surface coating**
- **Summary**

Background and Motivation

- **Electron emission** is important to **fundamental research** and various applications.



Trucchi, D. M., and Melosh, N. A.. Mrs Bulletin 42, no. 7, 488-492 (2017).

HOME > SCIENCE > VOL. 356, NO. 6333 > REAL-TIME SPECTRAL INTERFEROMETRY PROBES THE INTERNAL DYNAMICS OF FEMTOSECOND SOLITON...

RESEARCH ARTICLE

Real-time spectral interferometry probes the internal dynamics of femtosecond soliton molecules

G. HERINK, F. KURTZ, B. JALALI, D. R. SOLLI, AND C. ROPERS

SCIENCE • 7 Apr 2017 • Vol 356, Issue 6333 • pp. 50-54 • DOI:10.1126/science.aal5326

nature > nature physics > articles > article

Published: 06 November 2017

Phase ordering of charge density waves traced by ultrafast low-energy electron diffraction

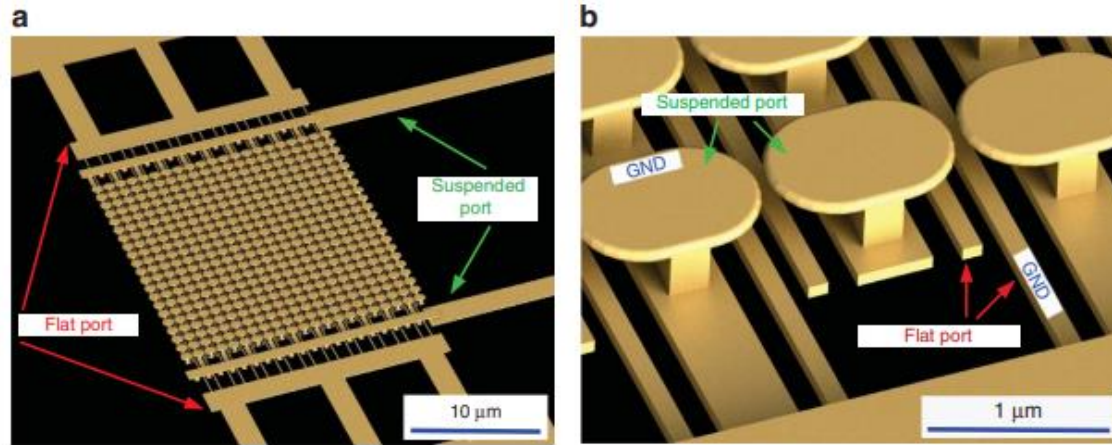
S. Vogelgesang, G. Storeck, J. G. Horstmann, T. Diekmann, M. Sivas, S. Schramm, K. Rossnagel, S. Schäfer & C. Ropers

Nature Physics 14, 184–190 (2018) | Cite this article

Background and Motivation

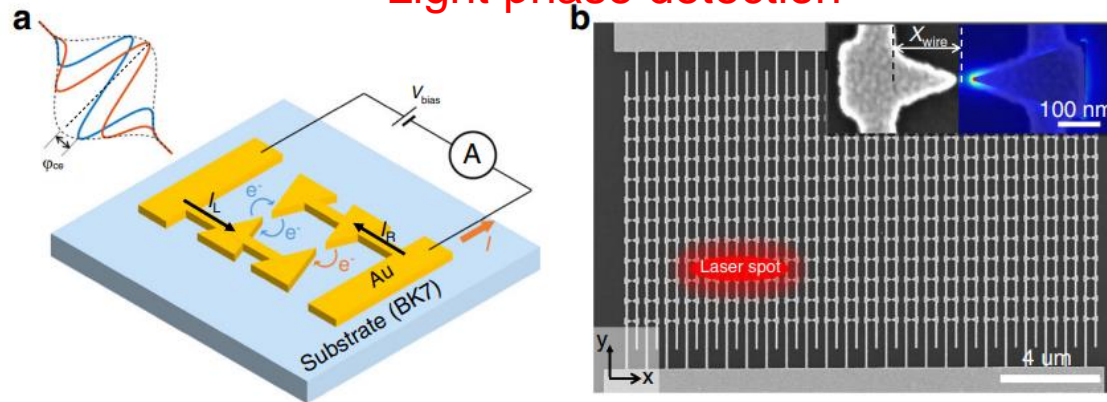
- **Electron emission** is important to fundamental research and **various applications**.

Photoemission-based device



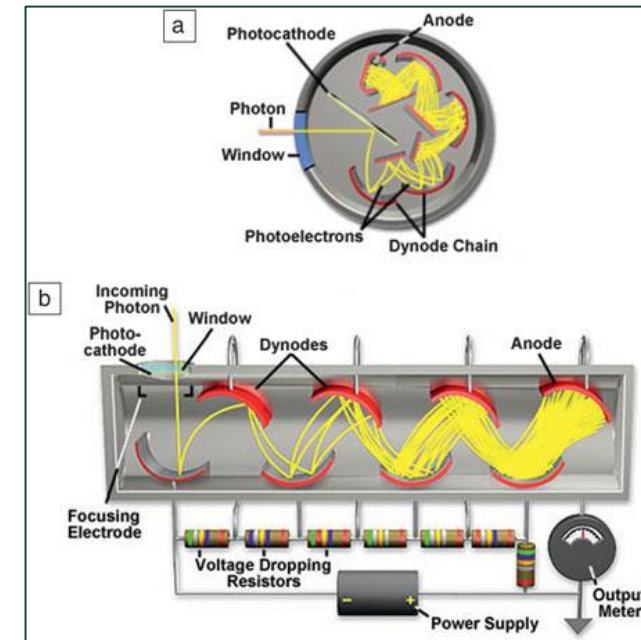
Forati, E., Dill, T.J., Tao, A.R. and Sievenpiper, D. *Nature communications*, 7(1), p.13399 (2016).

Light phase detection



Yang, Y., et al.. *Nature communications*, 11(1), p.3407 (2020).

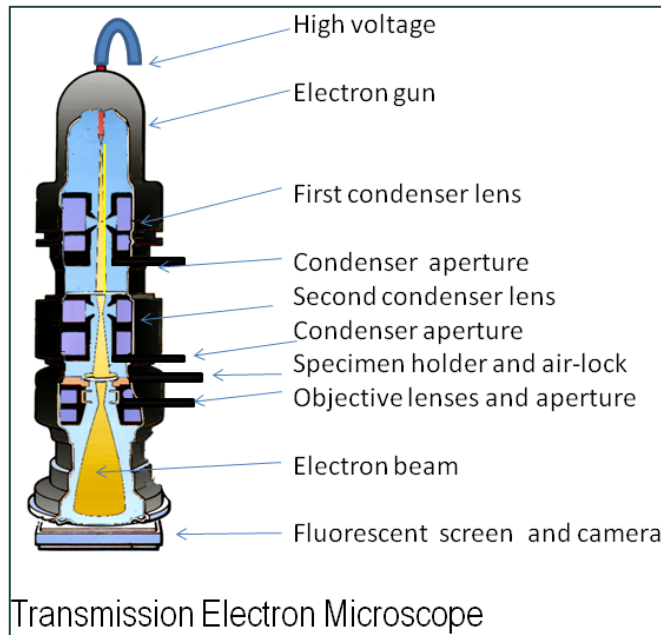
Photomultiplier



Trucchi, D. M., and Melosh, N. A.. *Mrs Bulletin* 42, no. 7, 488-492 (2017).

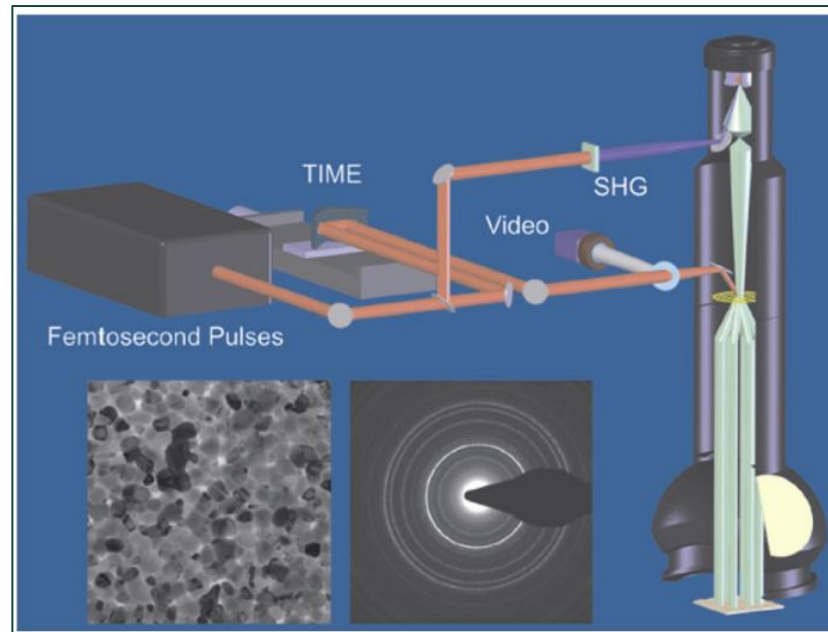
Background and Motivation

- **Electron emission** is important to fundamental research and **various applications**.



https://en.wikipedia.org/wiki/Electron_microscope#/media/File:Electron_Microscope.png

Ultrafast electron microscope



Grinolds, M.S., et al. *Proceedings of the National Academy of Sciences*, 103(49), pp.18427-18431 (2006).

Photocathode for accelerator

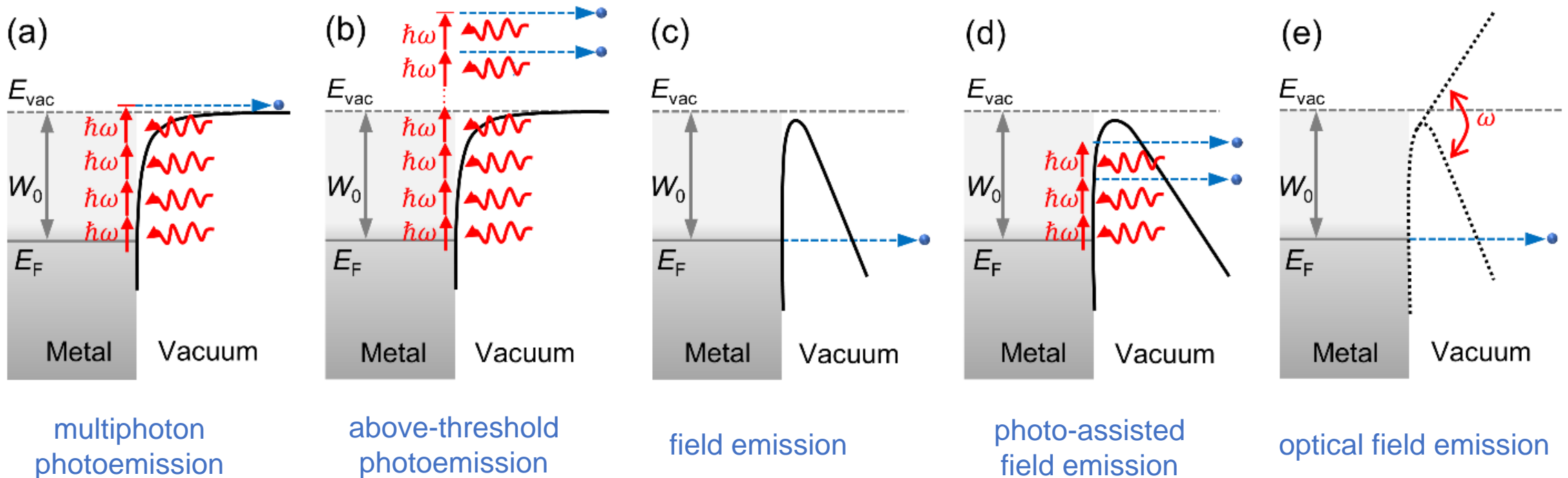


<https://web.physics.ucsb.edu/~smcbride/photocathodes/>

High quantum efficiency, low emittance, long lifetime, and short response time

Background and Motivation

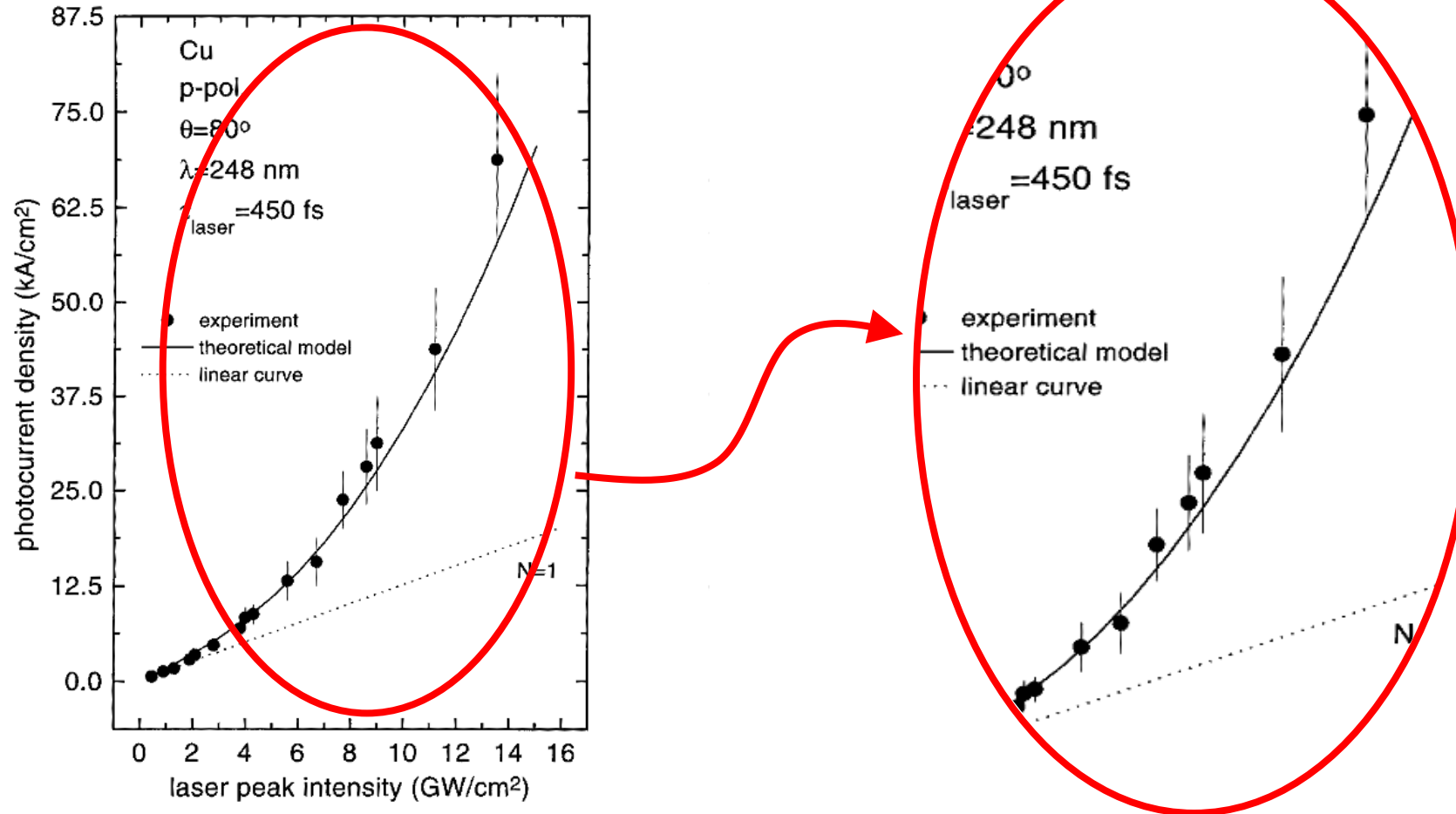
- Laser-matter interaction is primarily affected by **the laser wavelength**
 - a wide range of laser wavelength (~250 nm, ~800 nm, mid-infrared, THz)



electron emission mechanisms

Background and Motivation

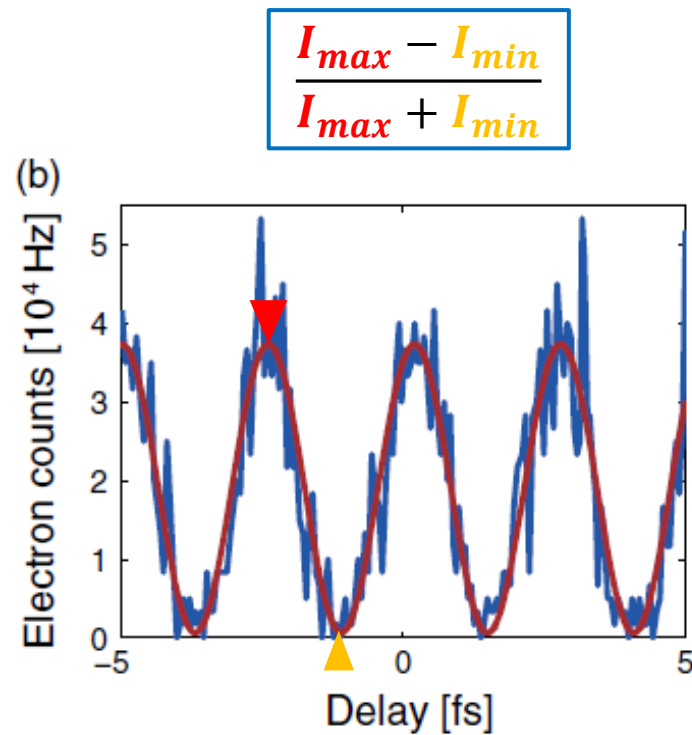
- Laser acts as a **heat source**



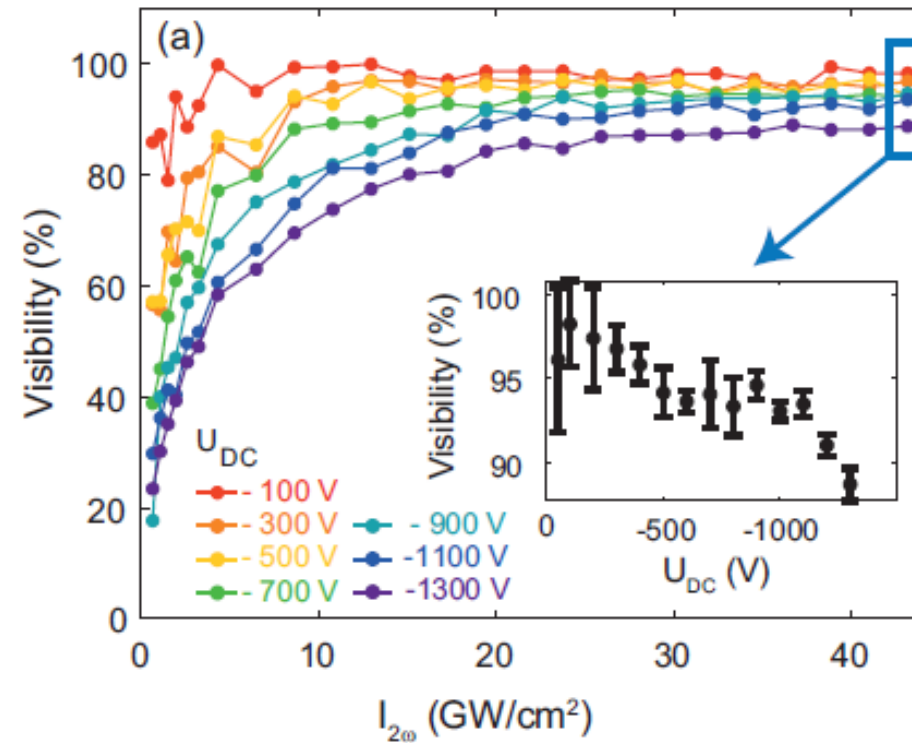
Papadogiannis, N. A., S. D. Moustazis, and J. P. Garreau-Montaut. *J. Phys. D: Appl. Phys* 30(17), 2389 (1997).

Background and Motivation

- **Two-color laser** coherent control of photoemission



Förster, M., et al. *Phys. Rev. Lett.* 117.21 (2016): 217601.

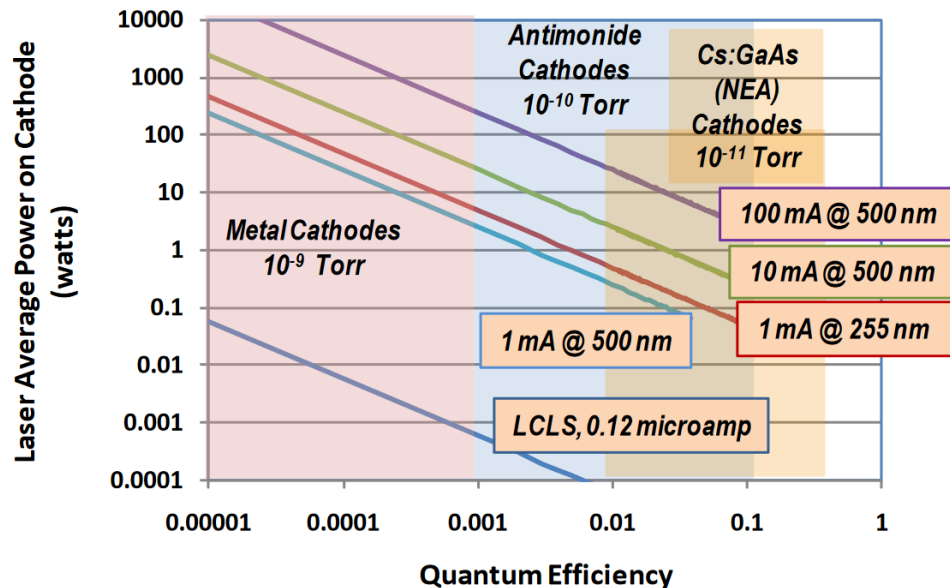


Dienstbier, Philip, Timo Paschen, and Peter Hommelhoff. *J. Phys. B: Atomic, Molecular and Optical Physics* 54.13 (2021): 134002.

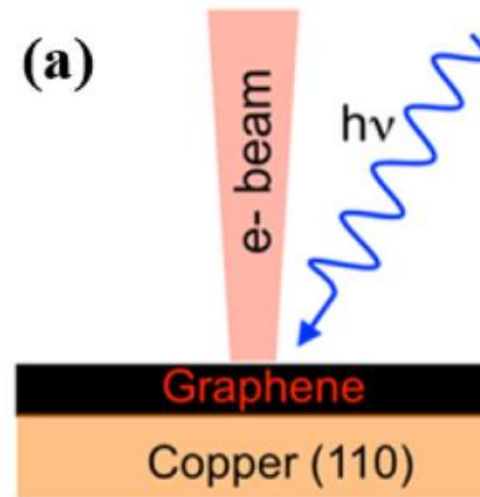
Two-color laser, DC field?

Background and Motivation

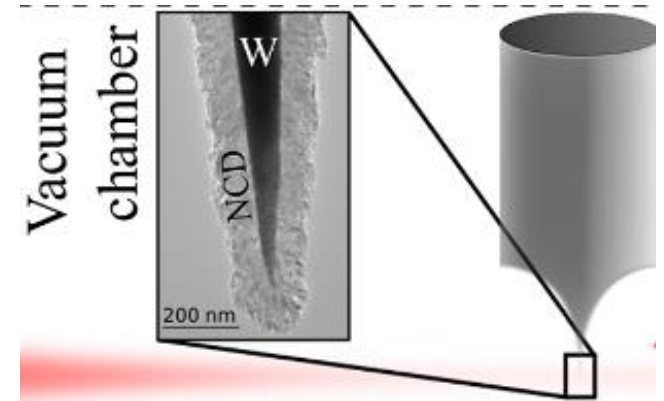
- **Cathode surface status** influences the fundamental mechanisms of photoemission
 - **Metals** and semiconductors
 - Artificial **coatings** (graphene, nano-diamond, silicon dioxide, and zinc dioxide)
 - Natural **coatings**: oxide



Dowell, D. H., et al. *Nuclear Instruments and Methods in Physics Research Section A: Accelerators, Spectrometers, Detectors and Associated Equipment* 622(3), 685-697 (2010).

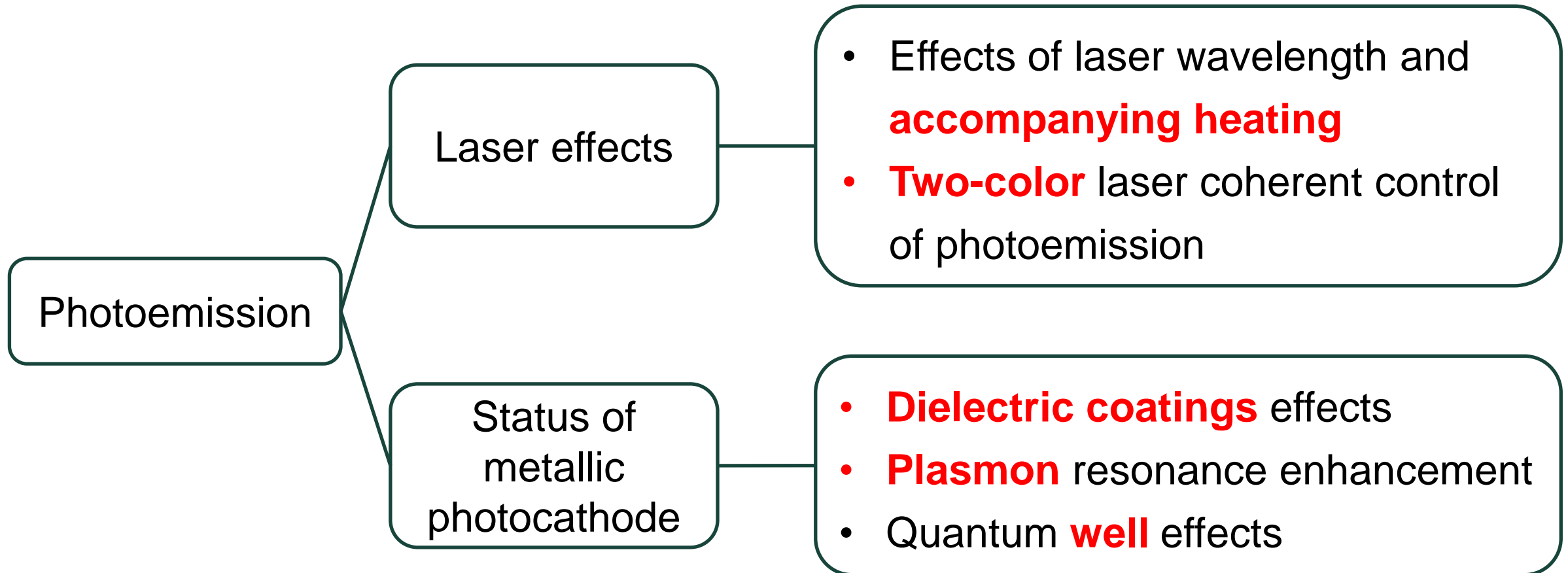


Liu, F., et al. *Applied Physics Letters*, 110(4), p.041607 (2017).

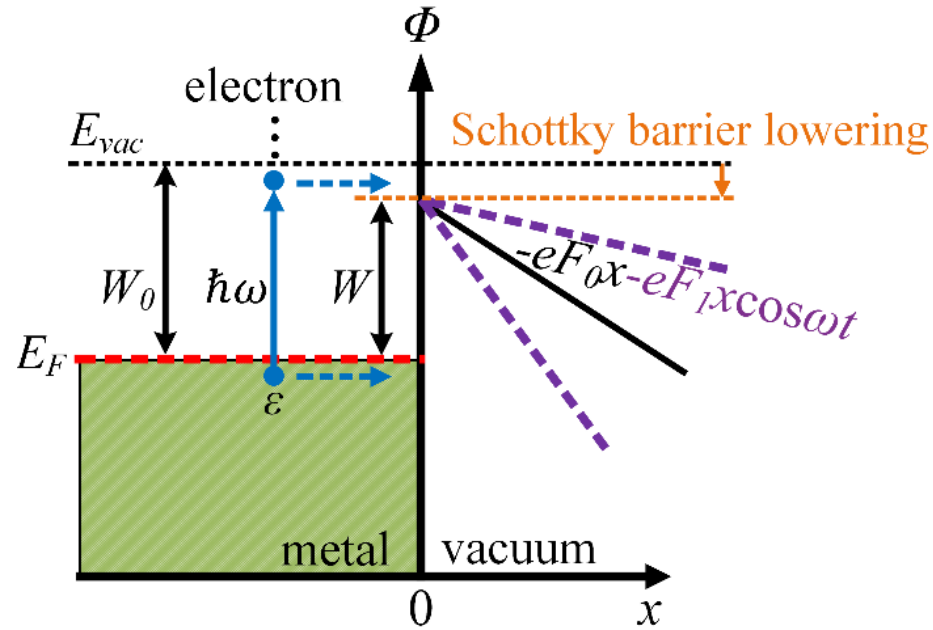


Tafel, A., Meier, S., Ristein, J. and Hommelhoff, P. *Physical Review Letters*, 123(14), p.146802 (2019).

Research Overview



Effects of laser wavelength & heating



E_{vac} : vacuum level
 W_0 : work function of metal
 E_F : Fermi energy
 ε : electron initial energy
 F_0 : dc field
 F_1 : laser field
 ω : laser frequency
 $W=W_0-W_{Schottky}$: effective work function

- Potential profile

$$\phi(x, t) = \begin{cases} 0, & x < 0 \\ E_F + W - eF_0x - eF_1x \cos \omega t, & x > 0 \end{cases}$$

- Schrödinger equation

$$i\hbar \frac{\partial \psi(x, t)}{\partial t} = -\frac{\hbar^2}{2m} \frac{\partial^2 \psi(x, t)}{\partial x^2} + \phi(x, t) \psi(x, t)$$

- Electron waves

$$\psi_I(x, t) = e^{-i\frac{\varepsilon}{\hbar}t + i\sqrt{\frac{2m\varepsilon}{\hbar^2}}x} + \sum_{n=-\infty}^{n=\infty} R_n e^{-i\frac{\varepsilon+n\hbar\omega}{\hbar}t - i\sqrt{\frac{2m(\varepsilon+n\hbar\omega)}{\hbar^2}}x}, x < 0$$

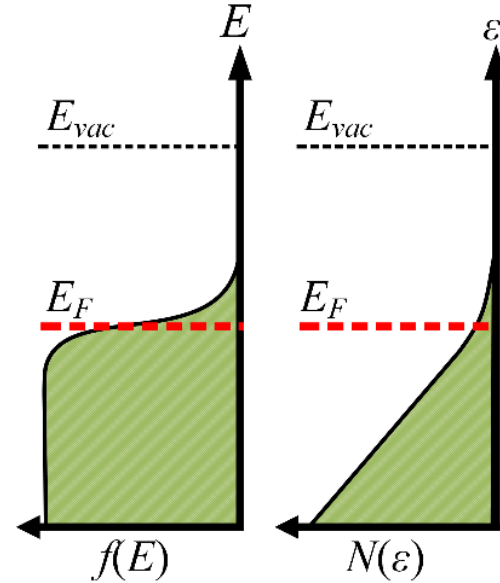
Effects of laser wavelength & heating

- Electron waves

$$\psi_{II}(x, t) = \sum_{n=-\infty}^{n=\infty} T_n e^{i\sqrt{\frac{2mE_n}{\hbar^2}}\xi} e^{-i\frac{\varepsilon+n\hbar\omega}{\hbar}t} e^{\frac{ieF_1 \sin \omega t}{\hbar\omega}x + \frac{ie^2F_1^2 \sin 2\omega t}{8\hbar m\omega^3}}, x \geq 0 \quad F_0 = 0$$

$$\psi_{II}(x, t) = \sum_{n=-\infty}^{n=\infty} T_n [Ai(-\eta_n) - iBi(-\eta_n)] \Gamma, x \geq 0 \quad F_0 \neq 0$$
 with $\Gamma = e^{i\sqrt{\frac{2mE_n}{\hbar^2}}\xi} e^{-i\frac{\varepsilon+n\hbar\omega}{\hbar}t} e^{\frac{ieF_1 \sin \omega t}{\hbar\omega}x + \frac{ie^2F_1^2 \sin 2\omega t}{8\hbar m\omega^3}} e^{-\frac{ie^2F_0F_1 \sin \omega t}{\hbar m\omega^3}}$
- Boundary conditions: ψ and $\partial\psi/\partial x$ continuous at the interface $\rightarrow R_n$ & T_n
- **Electron transmission probability** at electron initial energy ε is defined as $w(\varepsilon, x, t) = \frac{j_t}{j_i}$,
with $j = \frac{i\hbar}{2m} (\psi \nabla \psi^* - \psi^* \nabla \psi)$
- Time-averaged **electron transmission probability** $w_n(\varepsilon) = \begin{cases} \text{Im} \left(i \frac{\sqrt{\varepsilon + n\hbar\omega - V_0}}{\sqrt{\varepsilon}} |T_n|^2 \right), F_0 = 0 \\ \frac{1}{\pi} \left[\frac{eF_0\hbar}{\sqrt{2m}} \right]^{1/3} \frac{W^{1/3}}{\varepsilon}, F_0 \neq 0 \end{cases}$
- **Electron transmission probability:**
$$D(\varepsilon) = \sum_{n=-\infty}^{\infty} w_n(\varepsilon)$$

Effects of laser wavelength & heating



E_{vac} : vacuum level

E_F : Fermi energy

ε : electron longitudinal energy

E : electron energy, including both traverse and longitudinal energy

$f(E)$: Fermi-Dirac distribution

$$f(E) = \frac{1}{\exp\left(\frac{E - E_F}{k_B T}\right) + 1}$$

$N(\varepsilon)$: supply function $N(\varepsilon) = \frac{mk_B T}{2\pi^2 \hbar^3} \ln \left[1 + \exp\left(\frac{E_F - \varepsilon}{k_B T}\right) \right]$

- Emission current density

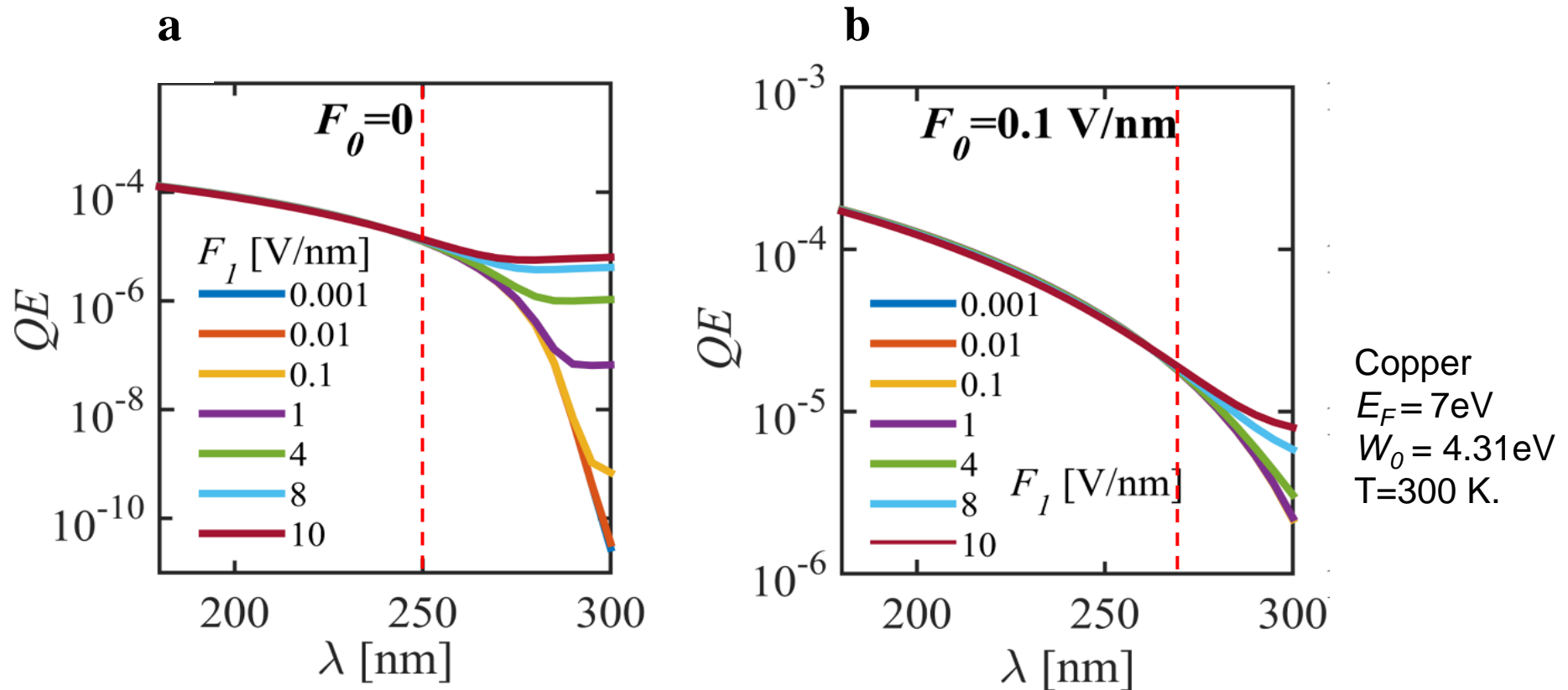
$$J = e \int_0^{\infty} D(\varepsilon) N(\varepsilon) d\varepsilon$$

where $N(\varepsilon)d\varepsilon$ is the number density of electrons inside metal with longitudinal energy between ε and $\varepsilon+d\varepsilon$ impinging on the surface of metal per unit time.

- The quantum efficiency (QE)

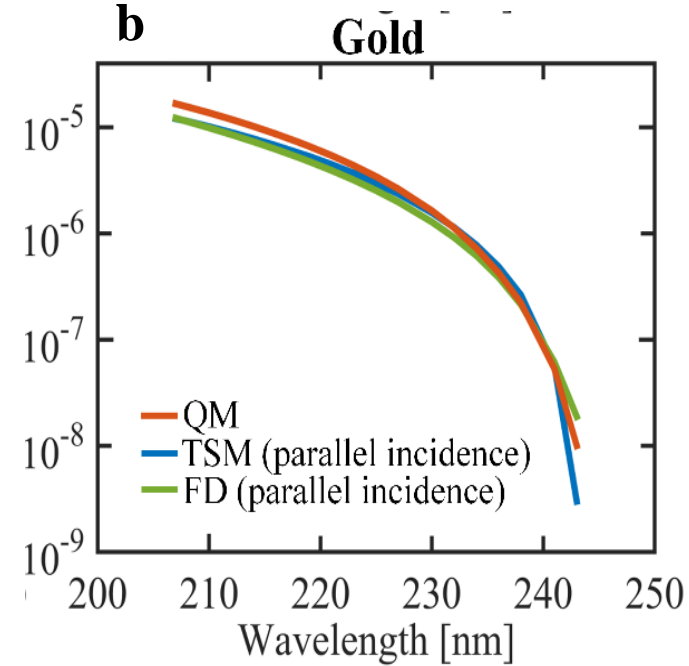
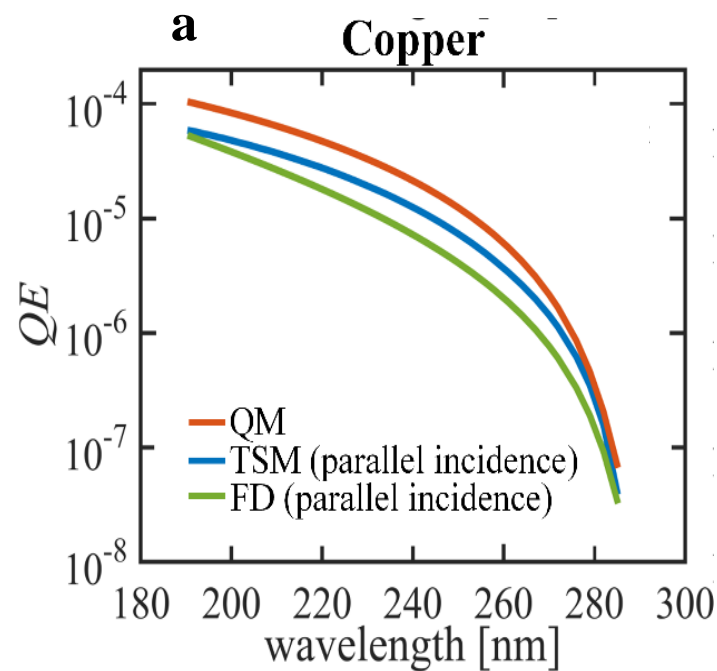
$$QE = \frac{J/e}{I/\hbar\omega}$$

Effects of laser wavelength & heating



$$I \propto F_1^{2n}, \quad QE \propto F_1^{2(n-1)}, \quad n = \left\langle \frac{W}{\hbar\omega} + 1 \right\rangle$$

Effects of laser wavelength & heating



$$F_1 = 0.01 \text{ V/nm}$$

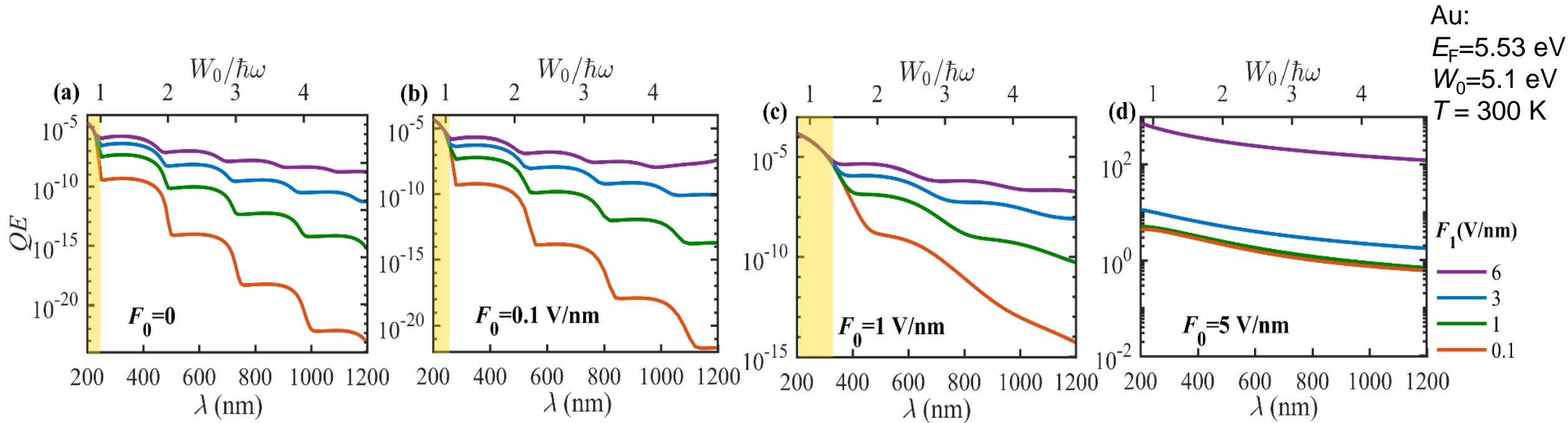
$$F_0 = 0$$

$$\text{FD: } QE(\omega) = a_1 \alpha A T^2 F\left(\frac{\hbar\omega - W}{k_B T}\right)$$

$$\text{TSM: } QE(\omega) = \alpha F_{e-e}(\omega) \frac{(E_F + \hbar\omega)}{2\hbar\omega} \left[1 + \frac{E_F + W}{E_F + \hbar\omega} - 2 \sqrt{\frac{E_F + W}{E_F + \hbar\omega}} \right]$$

$$\alpha = \frac{\pi \delta_s}{\lambda} \text{ for parallel incidence}$$

Effects of laser wavelength & heating



$$QE \propto F_1^{2(n-1)}, \quad n = \left\lfloor \frac{W}{\hbar\omega} + 1 \right\rfloor$$

- F_0 **shifts** step points and **smooths** curves
- Dominant **direct tunneling** for $F_0 = 5$ V/nm

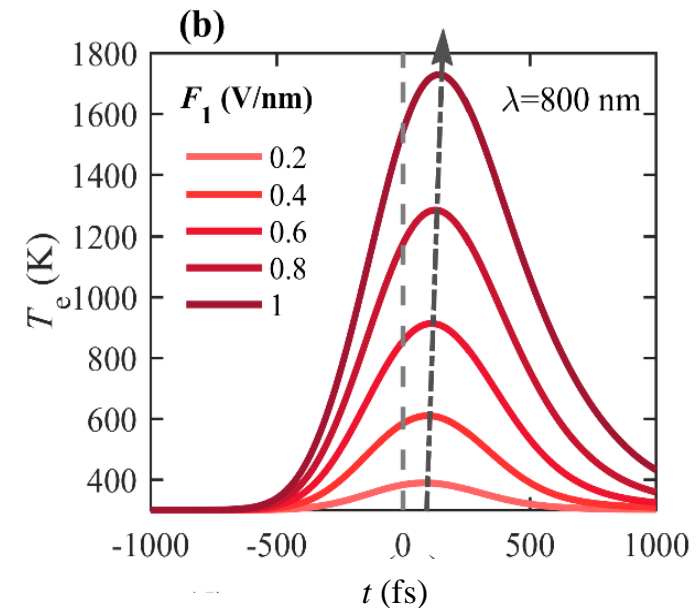
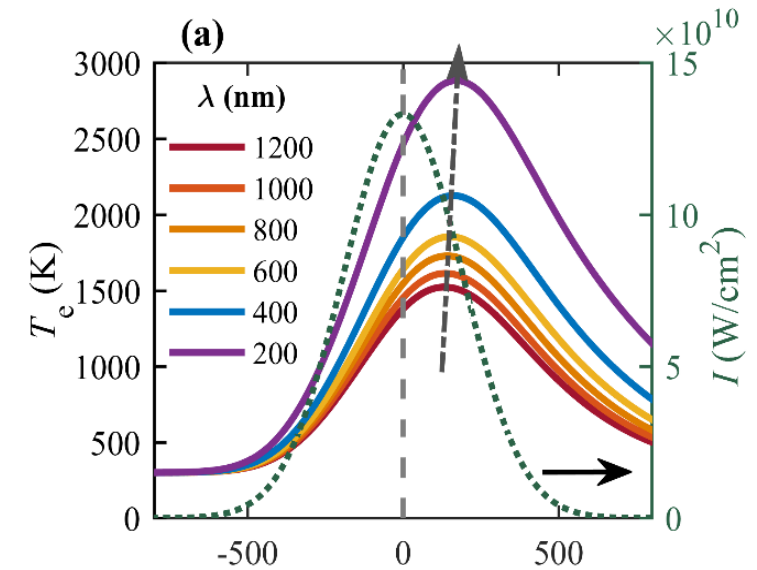
Effects of laser wavelength & heating

Two-temperature model

$$C_e \frac{\partial T_e}{\partial t} = \frac{\partial}{\partial x} \kappa \frac{\partial T_e(x, t)}{\partial x} - g(T_e - T_l) + G(x, t)$$

$$C_l \frac{\partial T_l}{\partial t} = g(T_e - T_l)$$

- C_e and C_l are the electron and lattice capacity;
- T_e and T_l are the electron and lattice temperature;
- g is the electron-lattice coupling coefficient;
- $G(x, t) = I(t)P_{abs}\alpha \exp(-\alpha x)$ is the energy absorbed by the metal;
- κ is the thermal conductivity.

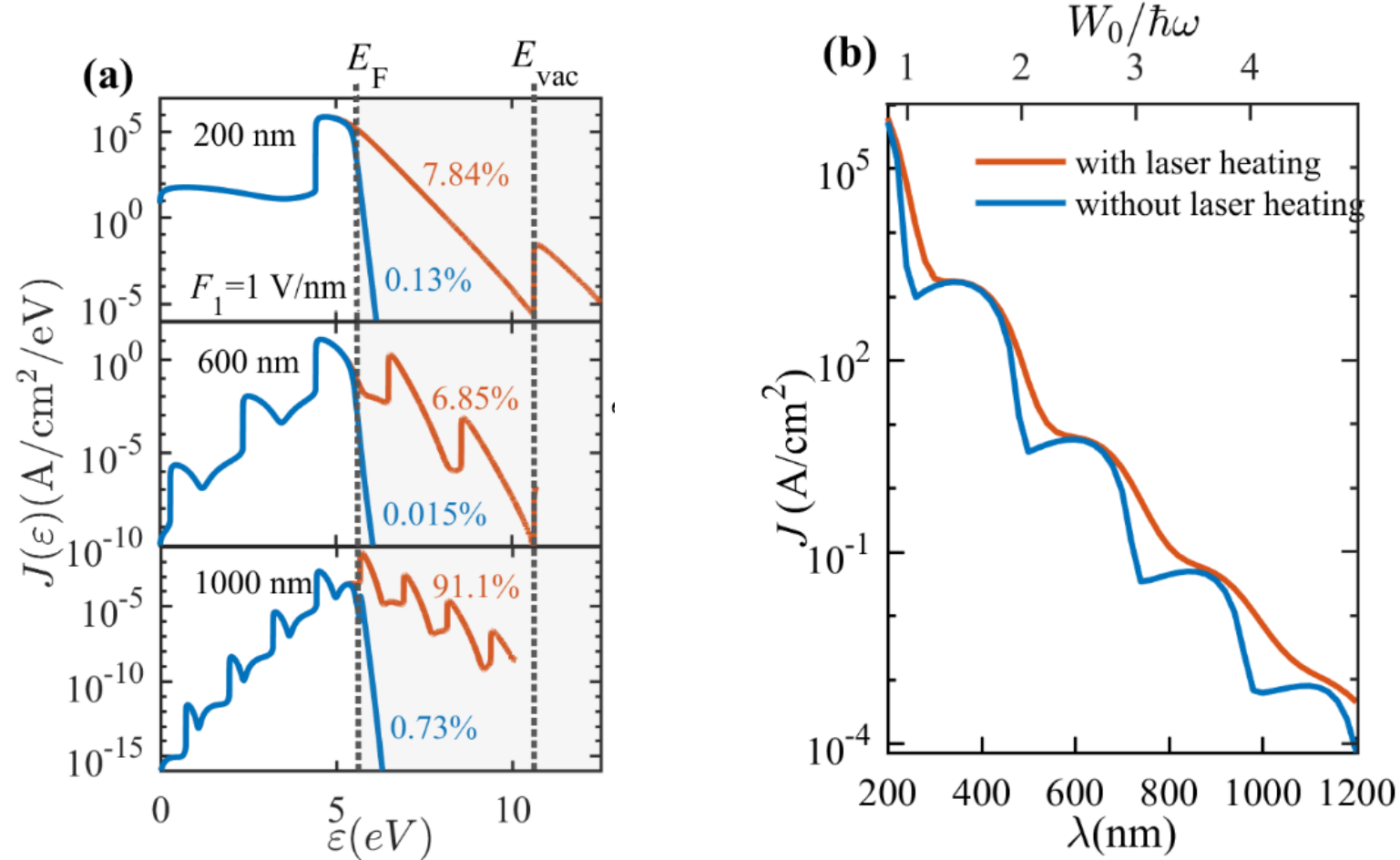


Effects of laser wavelength & heating

$$J(\varepsilon) = eD(\varepsilon)N(\varepsilon)$$

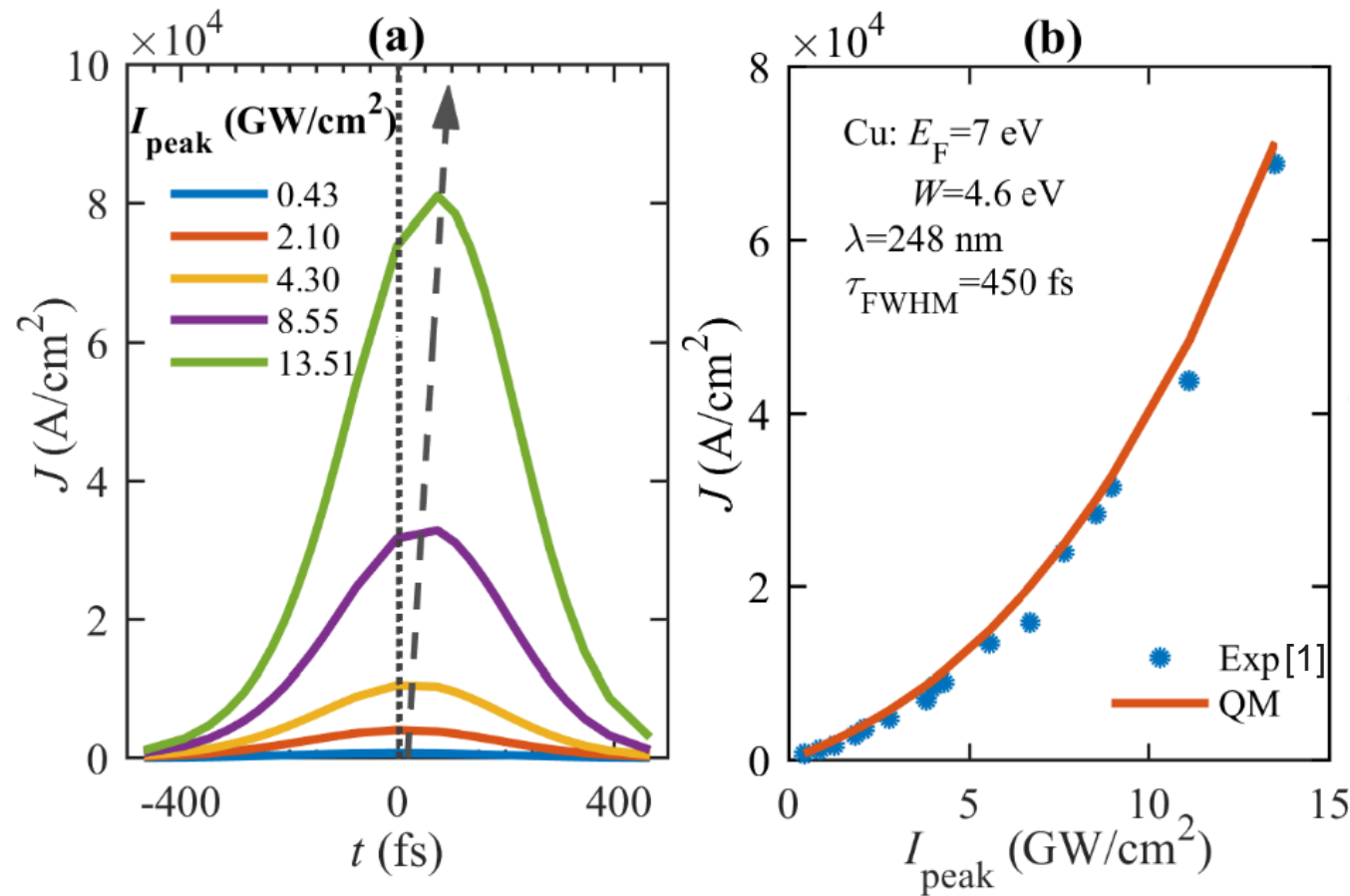
$$J = \int_0^{\infty} J(\varepsilon) d\varepsilon$$

$t = 0$



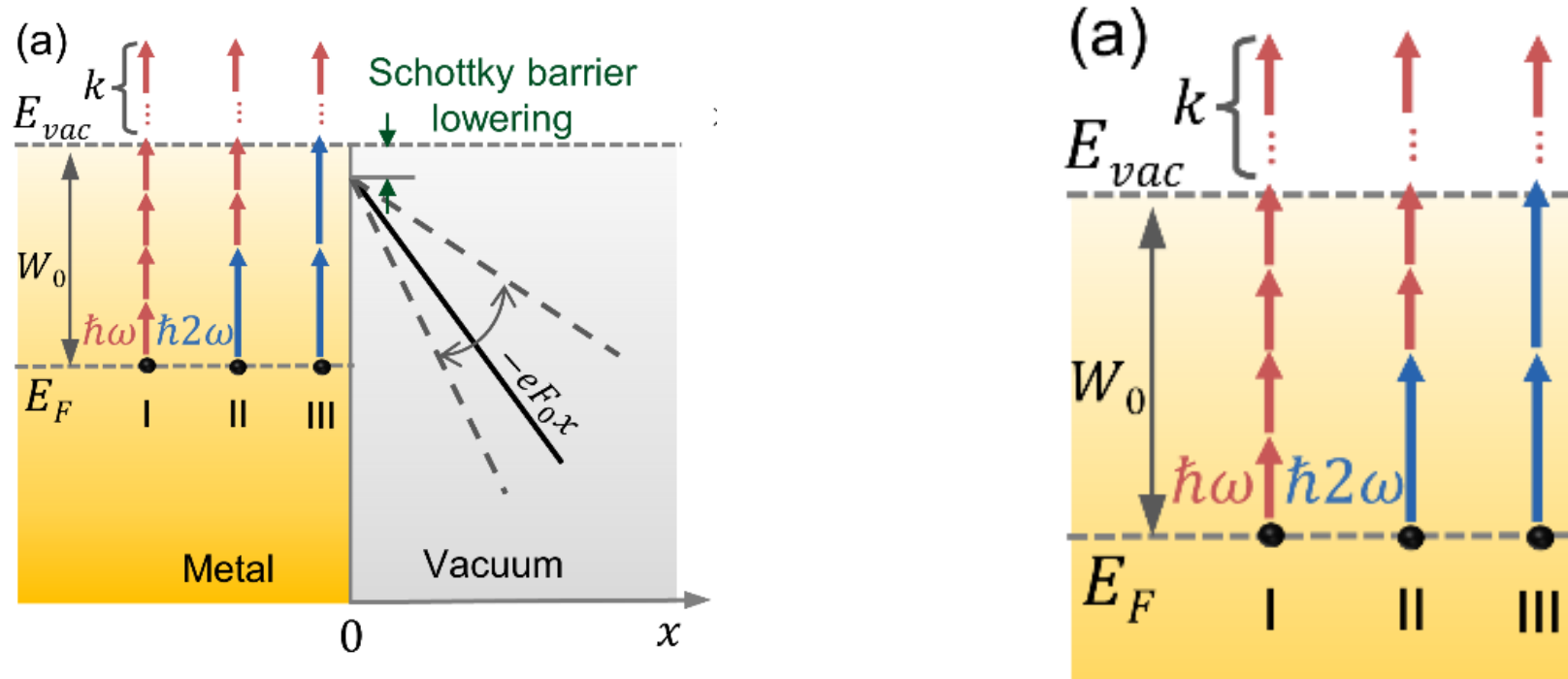
- Laser heating results in more electron emission from initial energy **above Fermi level**.
- Laser heating has greater effects at **step points** and **long laser wavelengths**.

Effects of laser wavelength & heating



- Good **agreement** with experimental results.
- **Lag** between emission current peak and laser intensity peak.

Two-color laser coherent control of photoemission



- Potential profile

$$\phi(x, t) = \begin{cases} 0, & x < 0 \\ V_0 - ef(t)x - eF_0x, & x \geq 0 \end{cases}$$

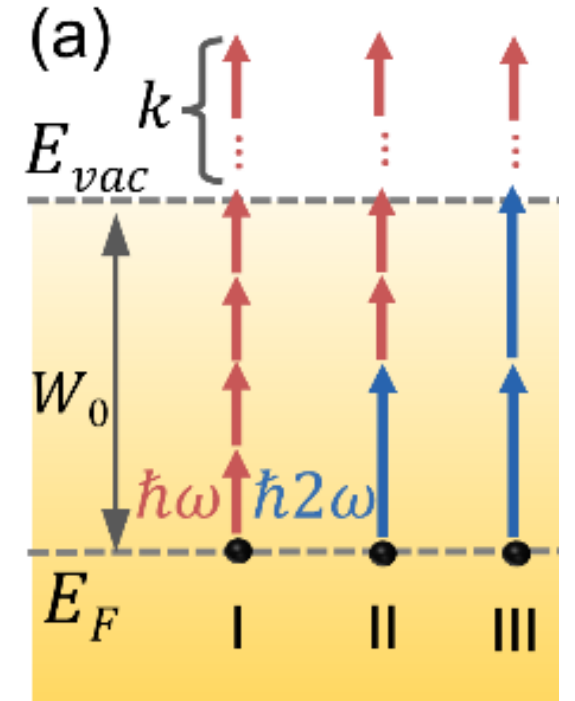
where $V_0 = E_F + W$, $W = W_0 - W_{Schottky}$, $f(t) = F_1 \cos(\omega t) + F_2 \cos(2\omega t + \theta)$

- Time-dependent Schrödinger equation

$$i\hbar \frac{\partial \psi(x, t)}{\partial t} = -\frac{\hbar^2}{2m} \frac{\partial^2 \psi(x)}{\partial x^2} + \phi(x, t)\psi(x)$$

Two-color laser coherent control of photoemission

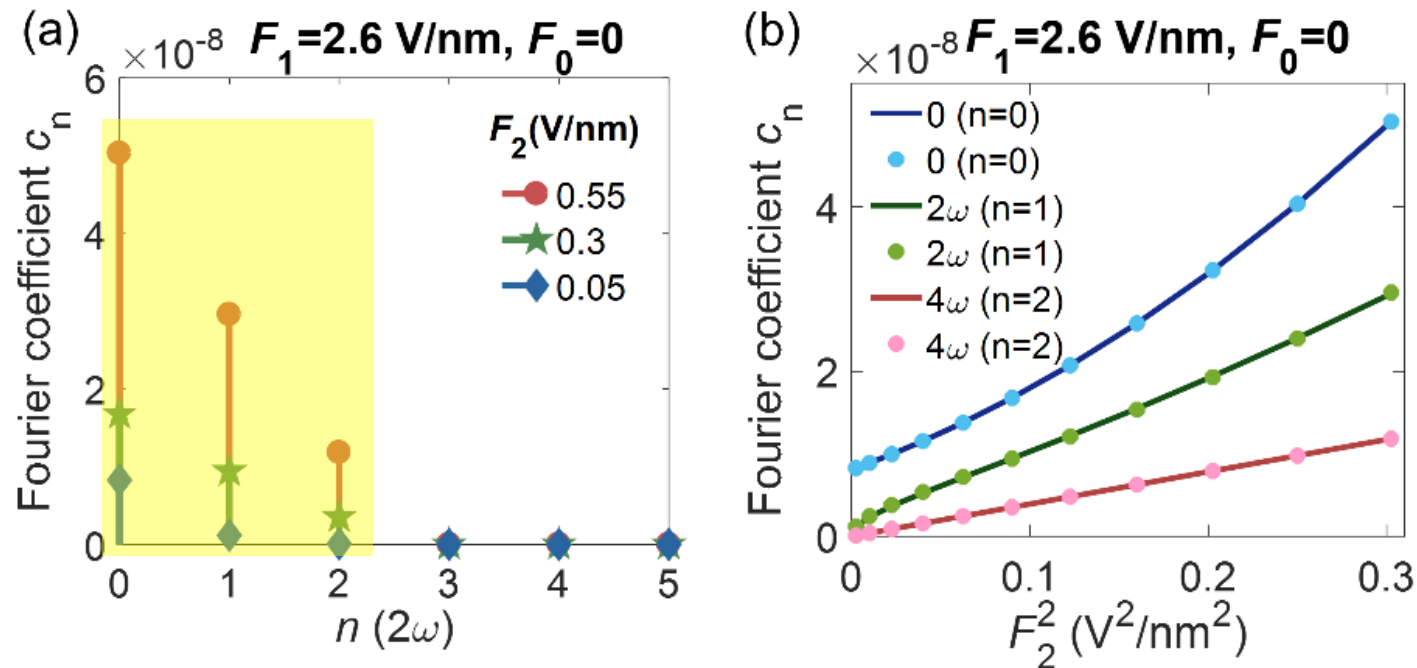
- $D_I \propto \alpha^k (F_1^2)^k (\alpha^4 (F_1^2)^4) = K_I$;
- $D_{II} \propto \alpha^k (F_1^2)^k (\zeta^2 (F_1^2)^2 F_2^2) = K_{II} F_2^2$;
- $D_{III} \propto \alpha^k (F_1^2)^k (\beta^2 (F_2^2)^2) = K_{III} (F_2^2)^2$;
- $D_{I\&II} \propto 2\sqrt{D_I D_{II}} \cos \theta \propto \alpha^k (F_1^2)^k (2\alpha^2 \zeta (F_1^2)^3 \sqrt{F_2^2} \cos \theta) = K_{I\&II} \sqrt{F_2^2} \cos(2\omega\tau)$;
- $D_{I\&III} \propto 2\sqrt{D_I D_{III}} \cos 2\theta \propto \alpha^k (F_1^2)^k (2\alpha^2 (F_1^2)^2 \beta F_2^2 \cos 2\theta) = K_{I\&III} F_2^2 \cos(4\omega\tau)$;
- $D_{II\&III} \propto 2\sqrt{D_{II} D_{III}} \cos \theta \propto \alpha^k (F_1^2)^k (2\zeta F_1^2 \beta \sqrt{(F_2^2)^3} \cos \theta) = K_{II\&III} \sqrt{(F_2^2)^3} \cos(2\omega\tau)$.



Two-color laser coherent control of photoemission

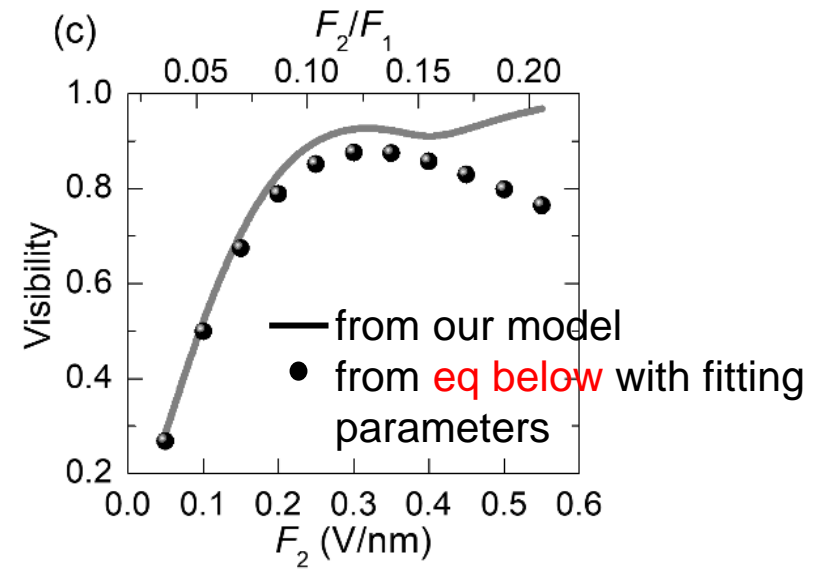
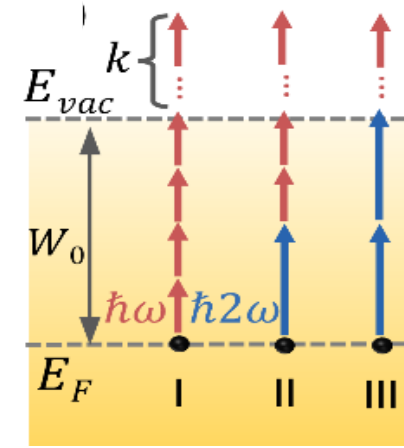
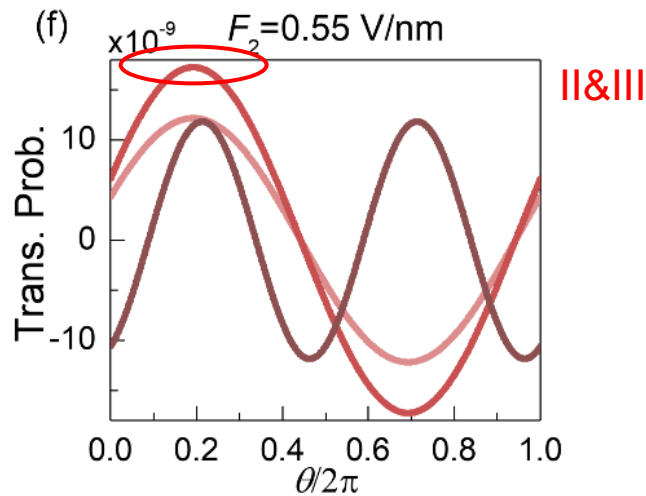
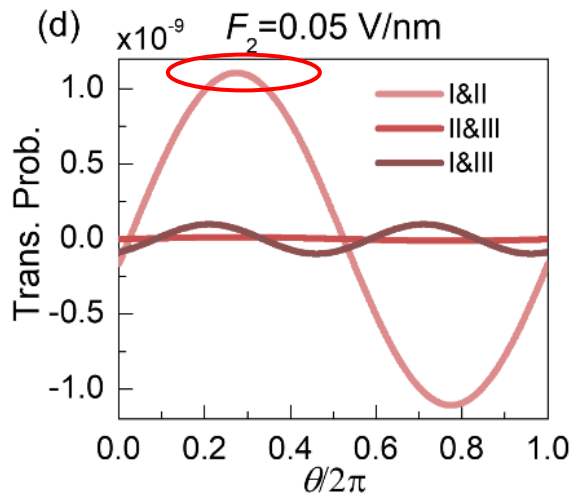
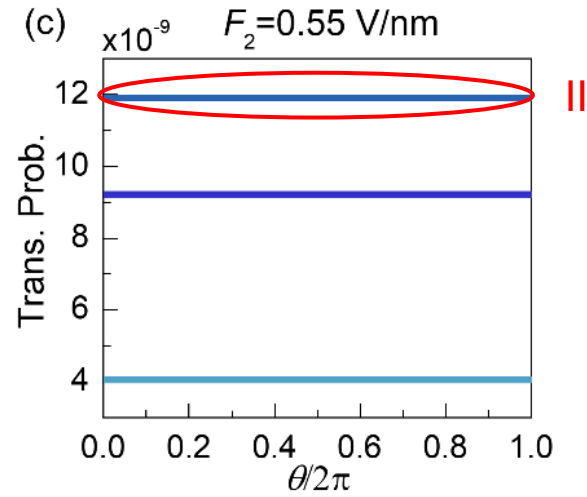
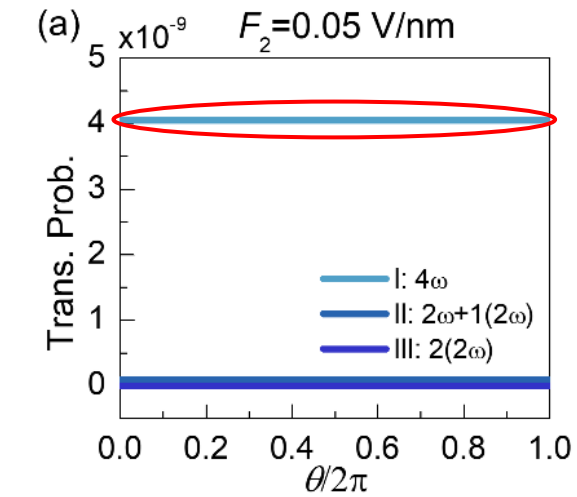
$$D(\tau) = \frac{c_0}{2} + \sum_{n=1}^N c_n \sin(n(2\omega)\tau + \varphi_n)$$

- with $c_0 = \frac{2}{T} \int_0^T D(\tau) d\tau$, $c_n = \sqrt{a_n^2 + b_n^2}$, $a_n = \frac{2}{T} \int_0^T D(\tau) \cos(n(2\omega)\tau) d\tau$, $b_n = \frac{2}{T} \int_0^T D(\tau) \sin(n(2\omega)\tau) d\tau$, $T = \frac{2\pi}{2\omega}$, and $\varphi_n = \tan^{-1}\left(\frac{a_n}{b_n}\right)$.



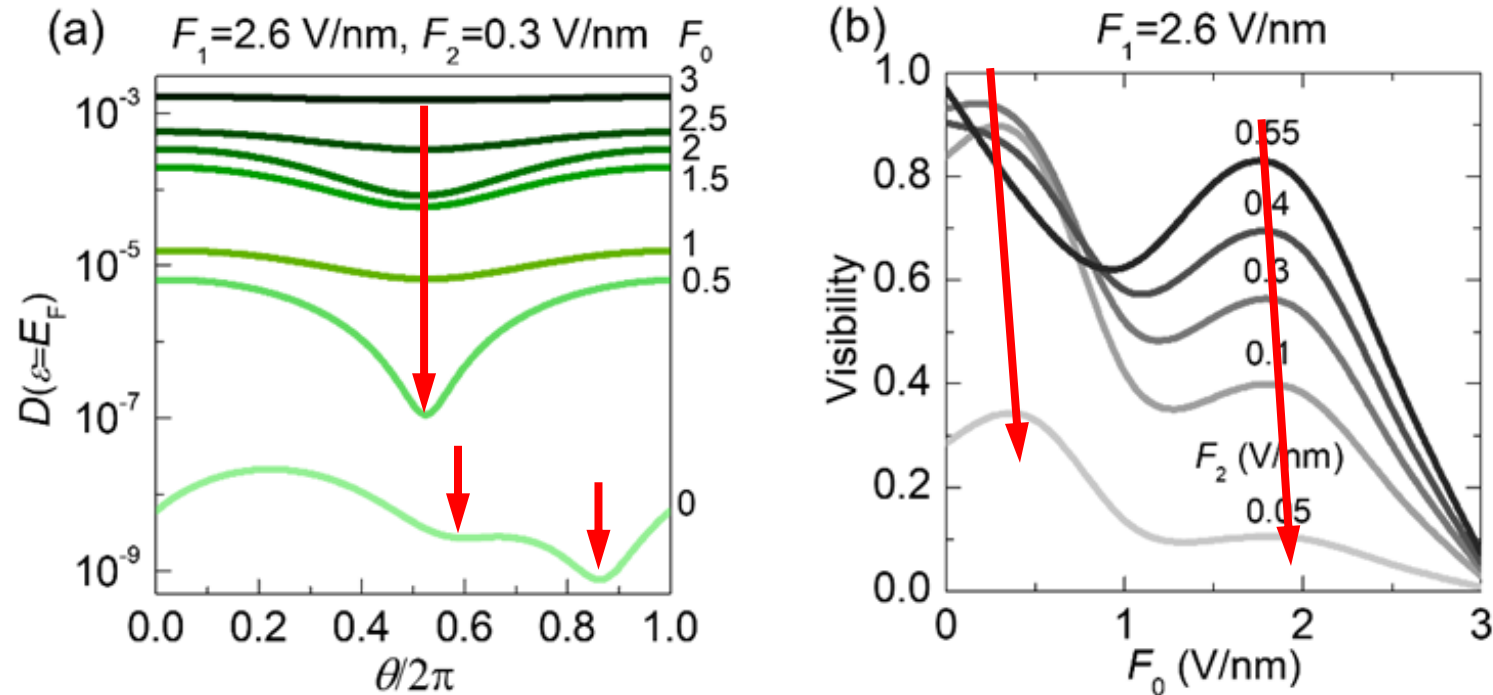
Two-color laser coherent control of photoemission

$$F_1 = 2.6 \text{ V/nm}, F_0 = 0$$



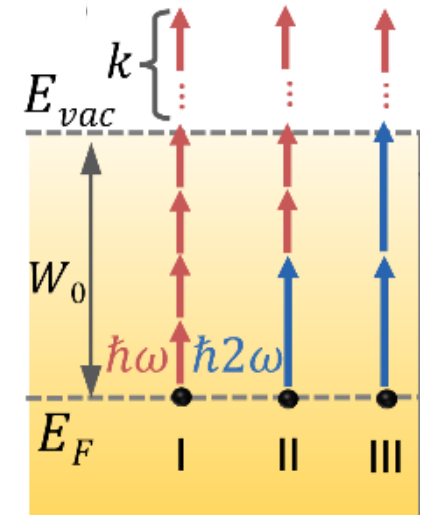
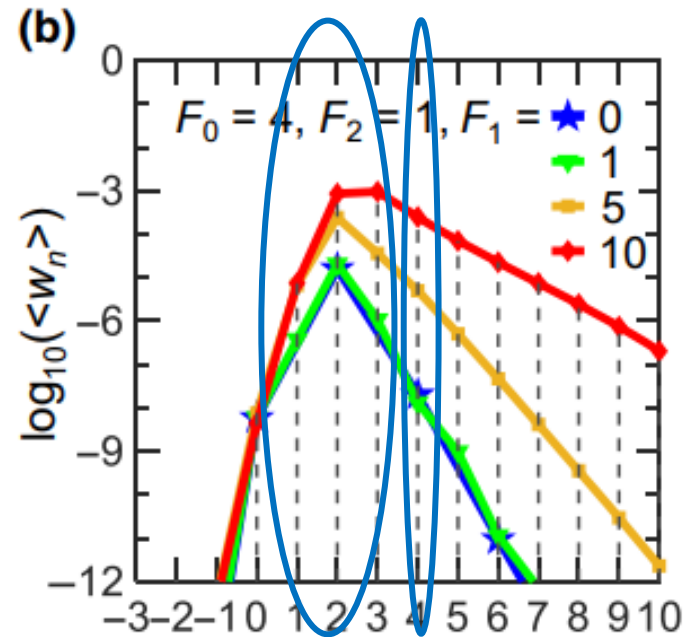
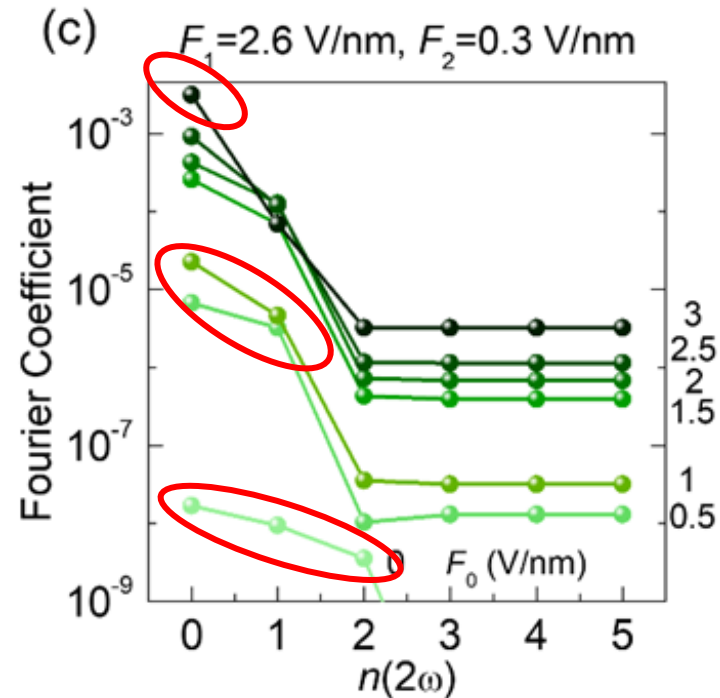
$$\text{Dots: } \frac{D_{I\&II}}{D_I + D_{II}}$$

Two-color laser coherent control of photoemission



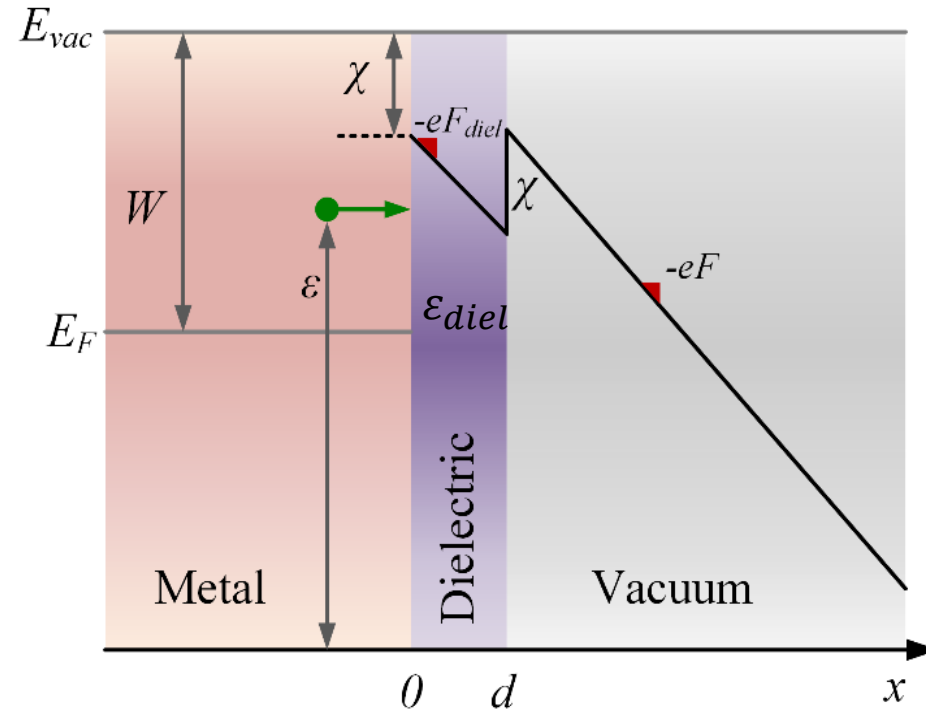
- DC field enhances electron emission
- Two peaks on visibility vs DC field

Two-color laser coherent control of photoemission



- Interference is sequentially suppressed as DC field increases

Effects of cathode surface coating



Potential profile

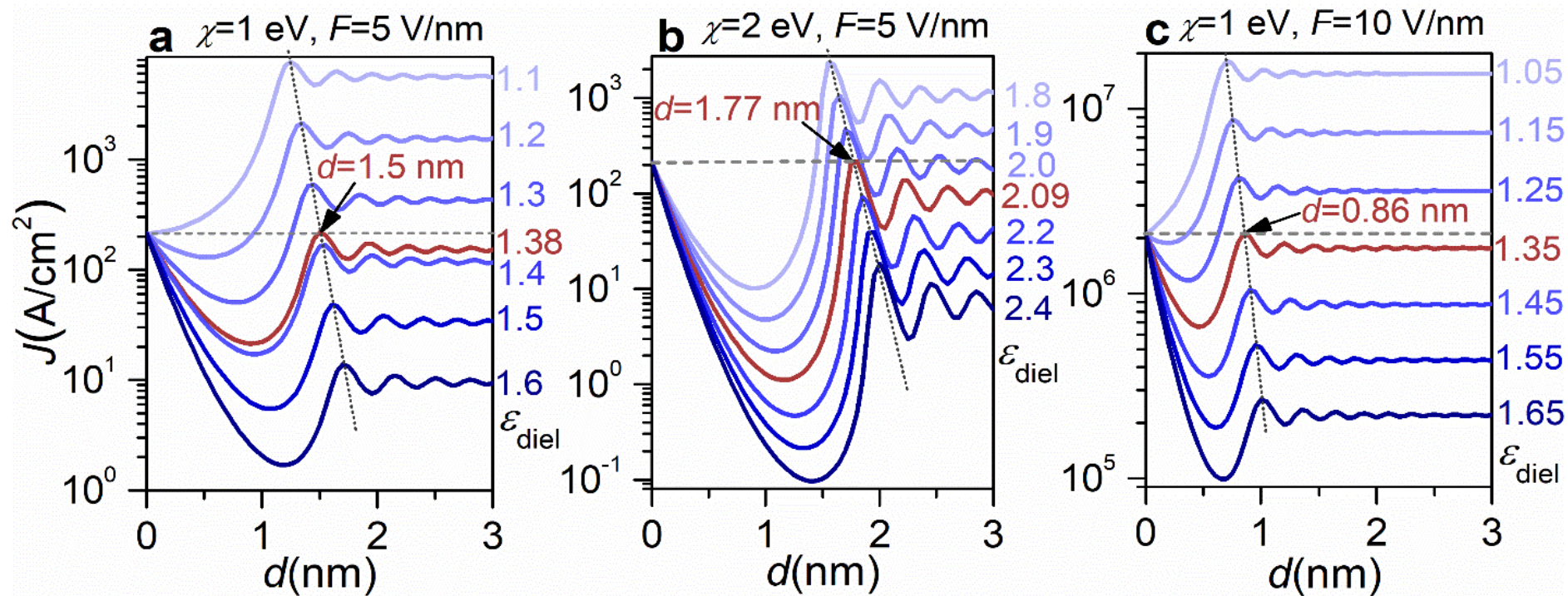
$$V(x) = \begin{cases} 0, & x < 0, \\ E_F + W - \chi - eF_{diel}x, & 0 \leq x < d, \\ E_F + W + e(F - F_{diel})d - eFx, & x \geq d. \end{cases}$$

Schrödinger equation

$$-\frac{\hbar^2}{2m} \frac{\partial^2}{\partial x^2} \psi(x) + [V(x) - \varepsilon] \psi(x) = 0$$

Complex wave

Effects of cathode surface coating

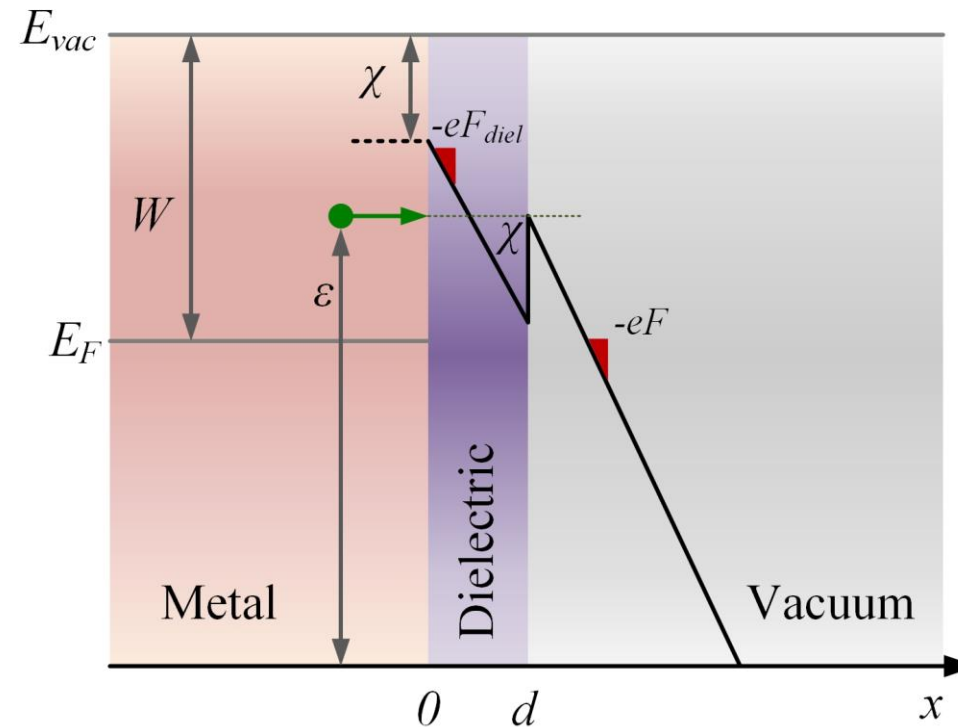


enhanced field emission

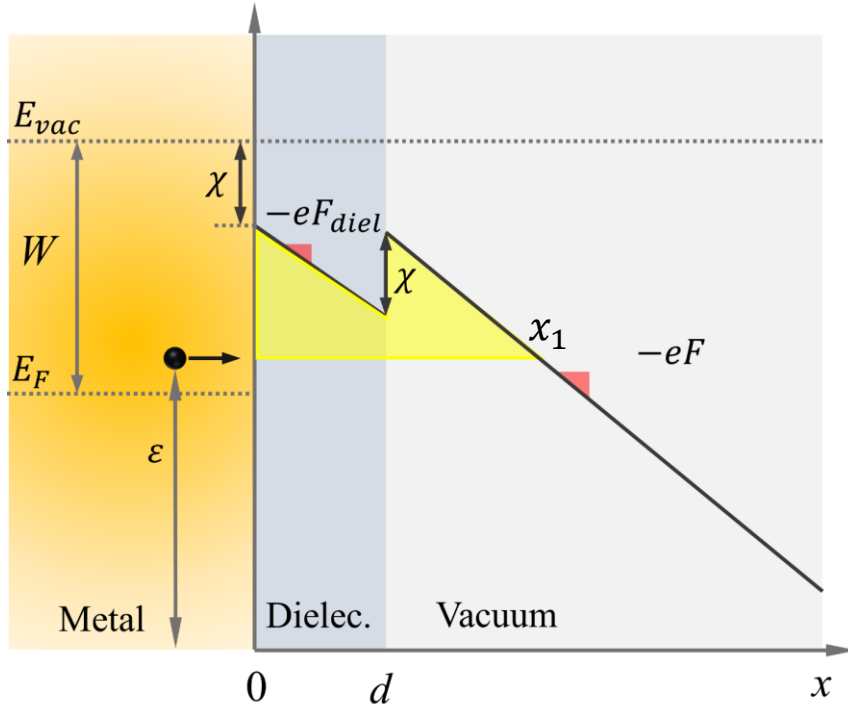
Effects of cathode surface coating

- An empirical relation between **thickness threshold** and **dielectric constant threshold** at room temperature

$$d_{th}[\text{nm}] = \frac{\varepsilon_{diel}^{th} W}{eF}$$



Effects of cathode surface coating



- Electron transmission probability

$$D(\varepsilon) = \exp[Q(\varepsilon)]$$

with $Q(\varepsilon) = -2 \int_0^{x_1} \sqrt{\frac{2m}{\hbar^2} [V(x) - \varepsilon]} dx$ by **WKBJ approximation**

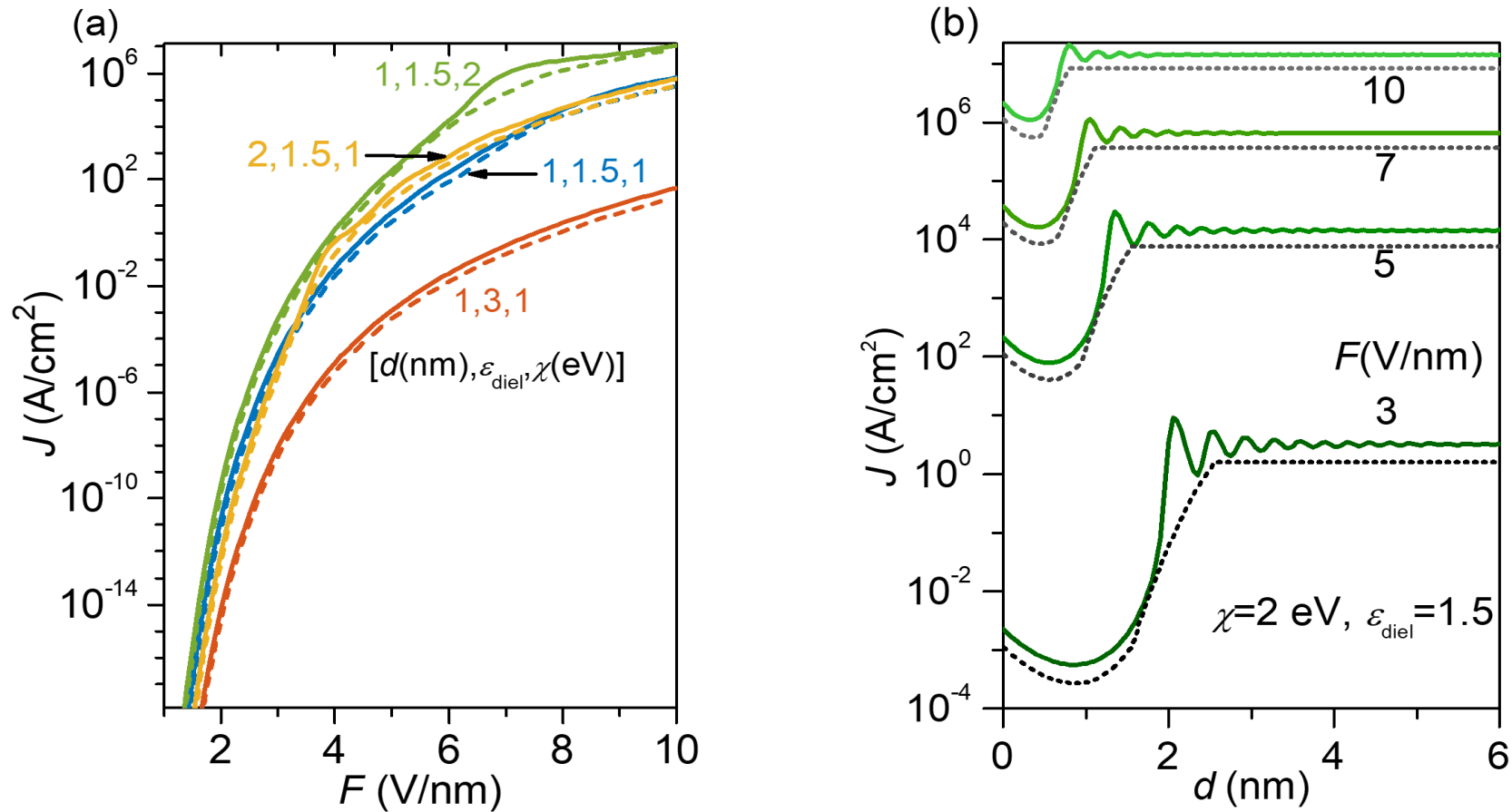
- Electron emission current density

$$J = e \int_0^{\infty} D(\varepsilon) N(\varepsilon) d\varepsilon$$

with $N(\varepsilon)$ the supply function

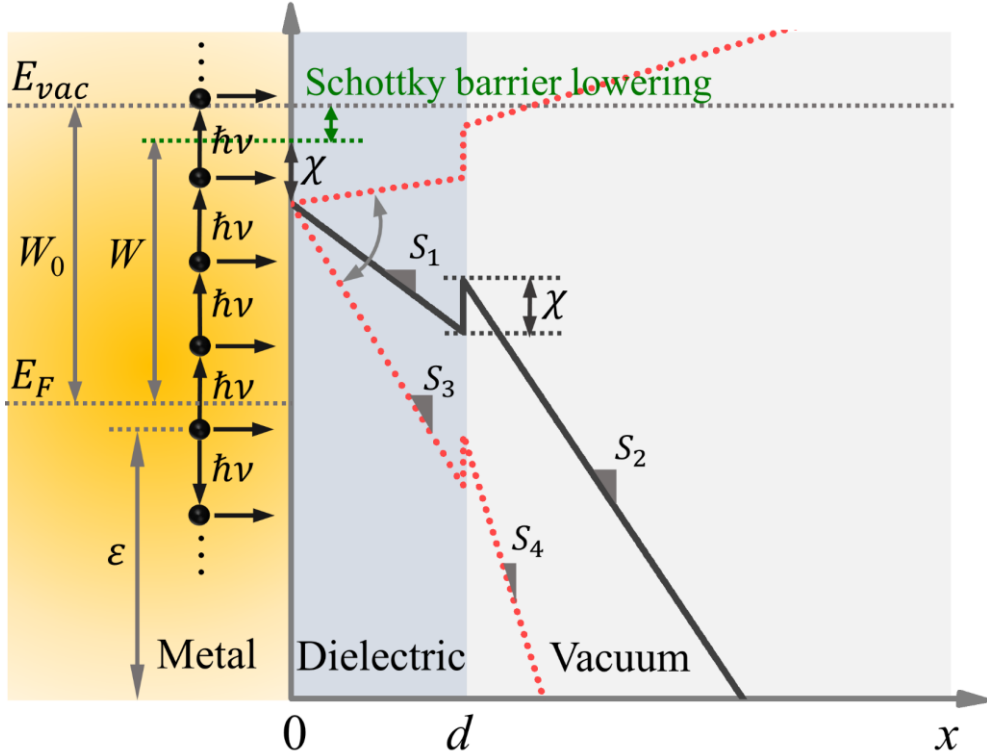
$$N(\varepsilon) = \frac{mk_B T}{2\pi^2 \hbar^3} \ln \left[1 + \exp \left(\frac{E_F - \varepsilon}{k_B T} \right) \right]$$

Effects of cathode surface coating



- Good **agreement** in the scaling
- Resonance behavior in J vs. d cannot be revealed by the modified FN equation

Effects of cathode surface coating

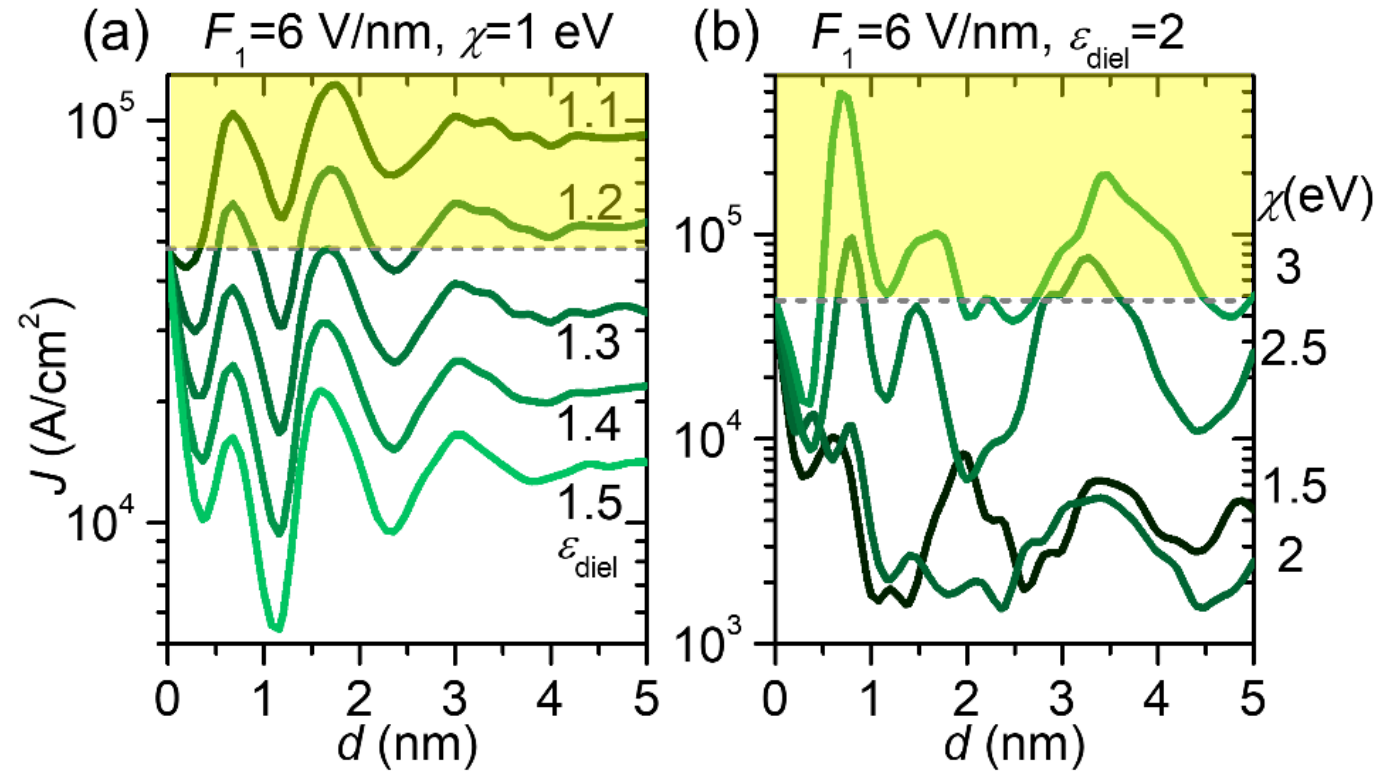


- Potential profile

$$\phi(x, t) = \begin{cases} 0, & x < 0, \\ E_F + W - \chi - eF_0^{diel}x - eF_1^{diel}x \cos \omega t, & 0 \leq x < d, \\ E_F + W + e(F_0 - F_0^{diel})d + e(F_1 - F_1^{diel})d \cos \omega t - eF_0x - eF_1x \cos \omega t, & x \geq d. \end{cases}$$

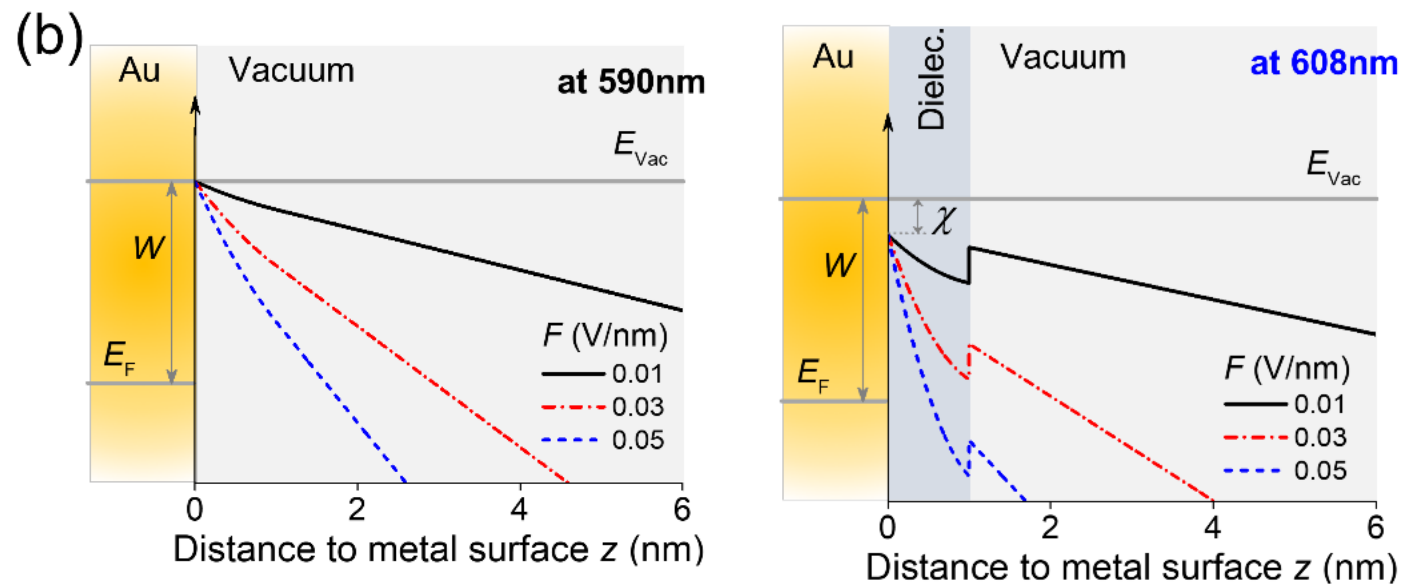
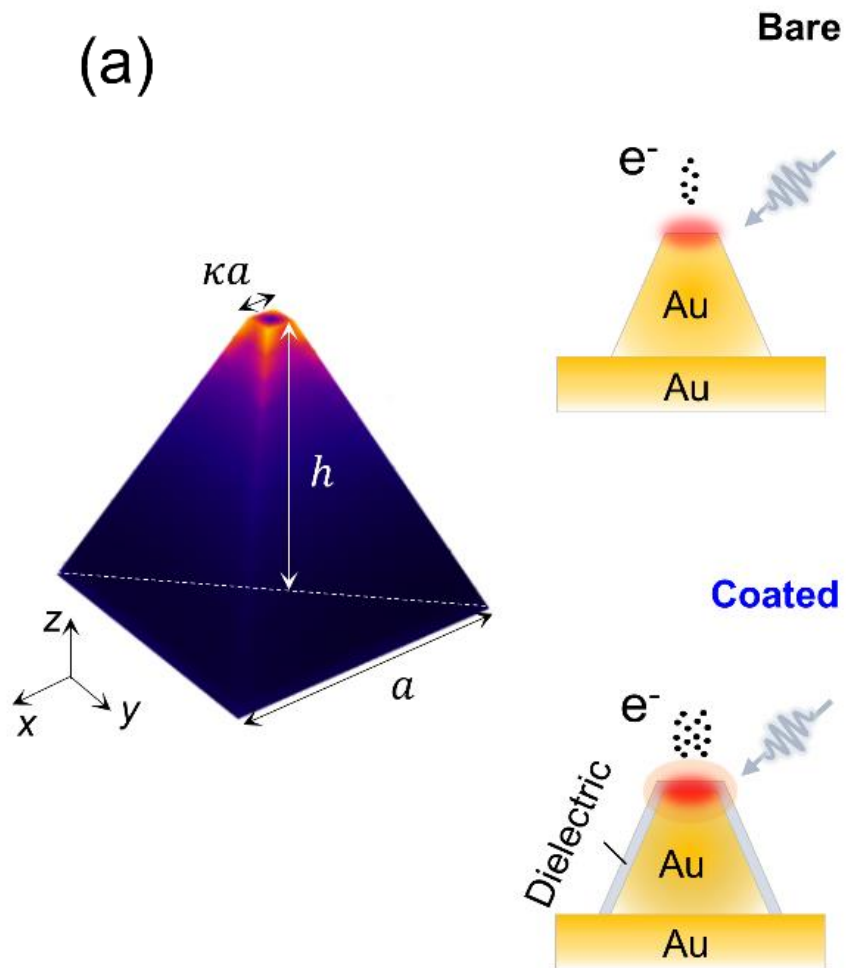
$W = W_0 - \Delta W$, ΔW is the Schottky barrier lowering. $F_1^{diel} = F_1/\epsilon_{diel}$, $F_0^{diel} = F_0/\epsilon_{diel}$ for a perfectly flat surface

Effects of cathode surface coating



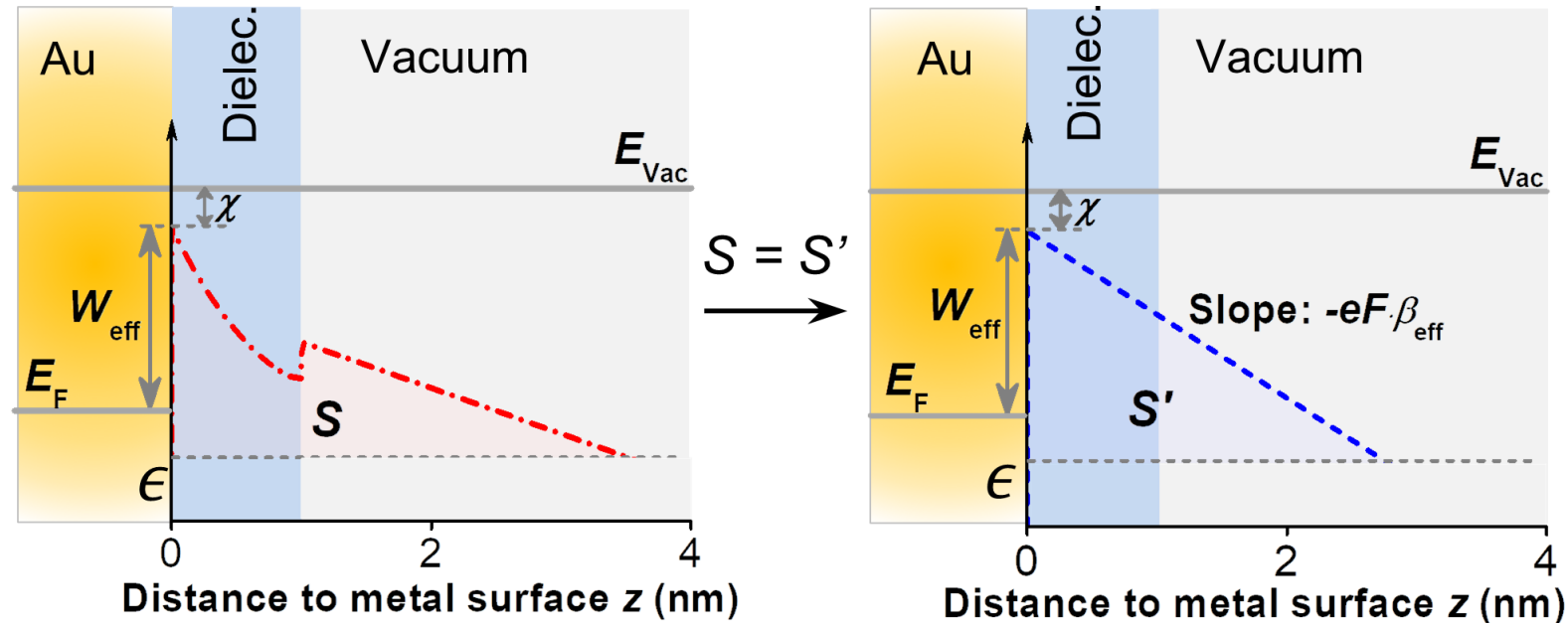
enhanced photoemission

Plasmon resonance enhancement



potential profile

Plasmon resonance enhancement

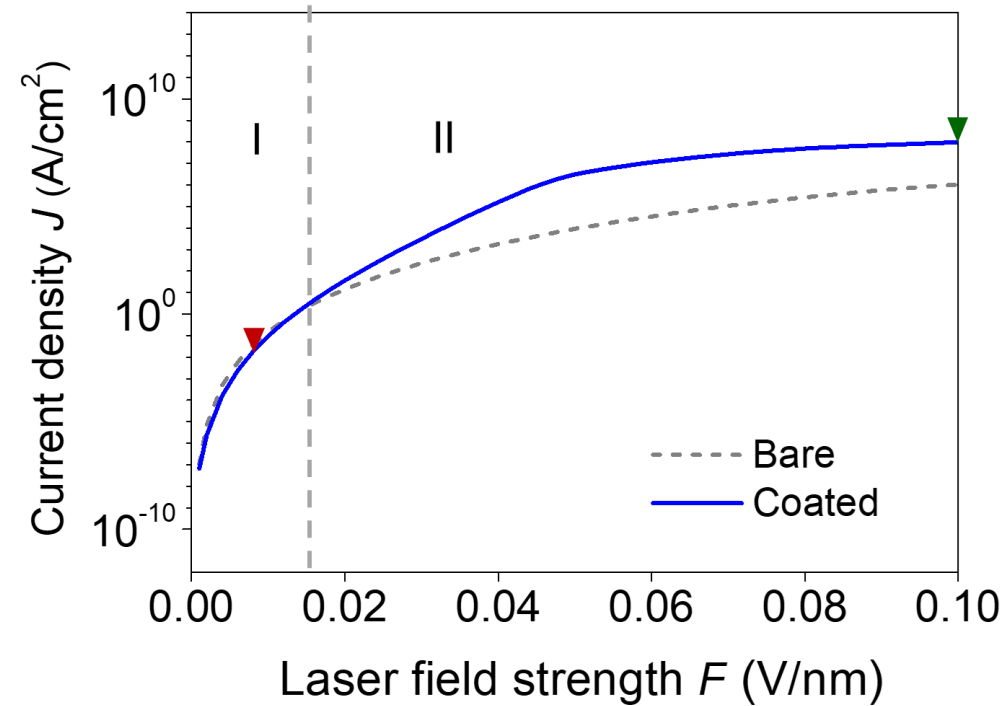


Effective barrier profile approximation

$$\phi(z, t) = \begin{cases} 0, & z < 0 \\ E_F + W_{eff} - e\beta_{eff}Fz \cos \omega t, & z > 0 \end{cases}$$

with $W_{eff} = W - \chi$

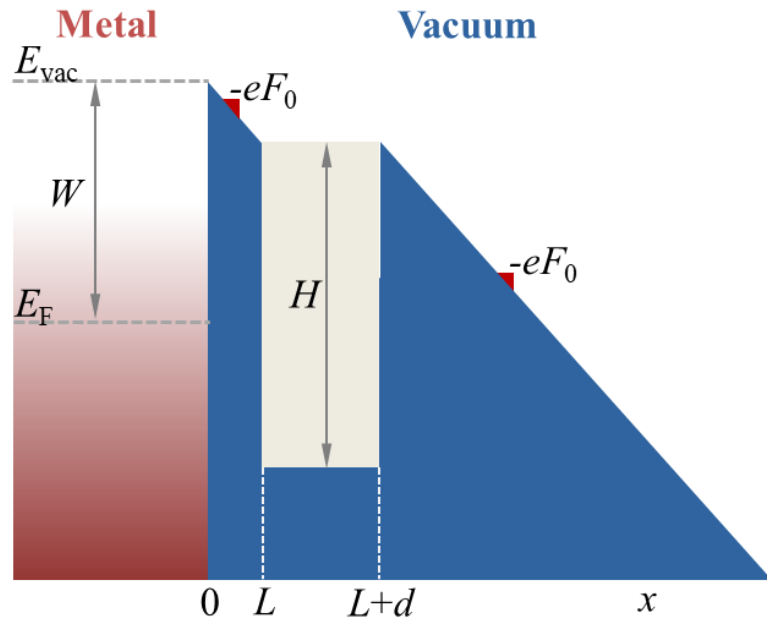
Plasmon resonance enhancement



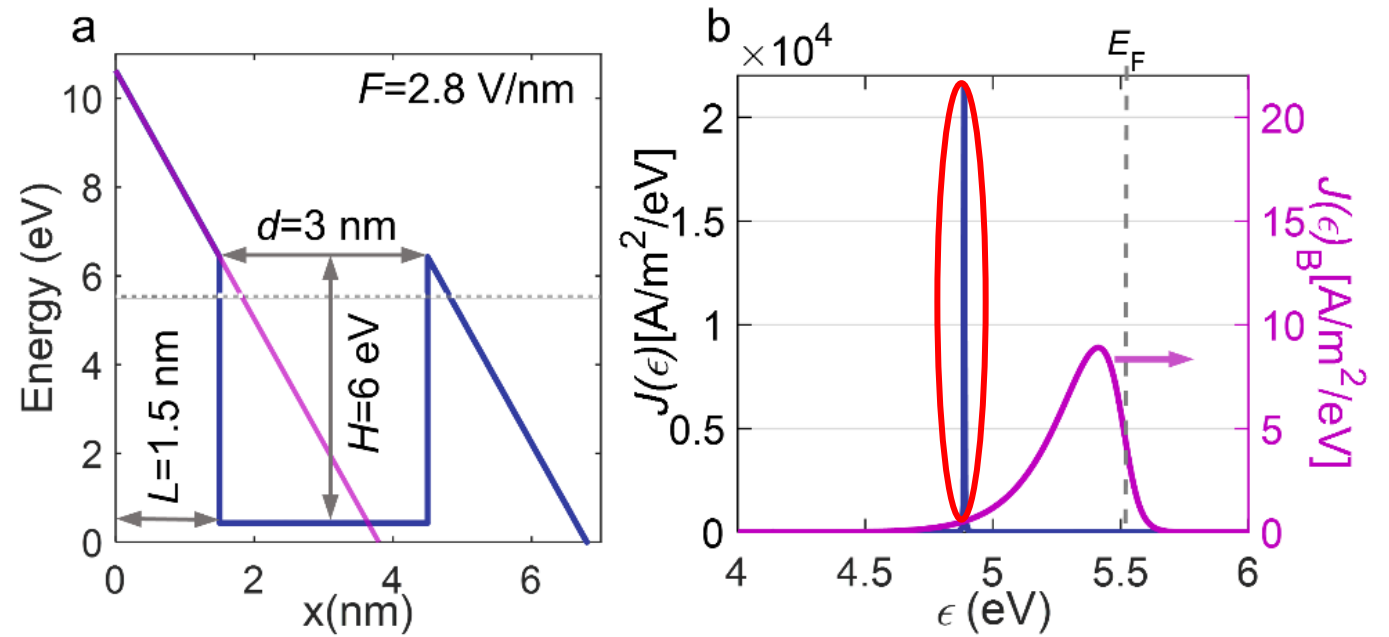
~2 orders of magnitude enhancement

Metal Surfaces with a Quantum Well

- Nanostructures or adsorbates (ions, atoms, or molecules etc.) on cathodes



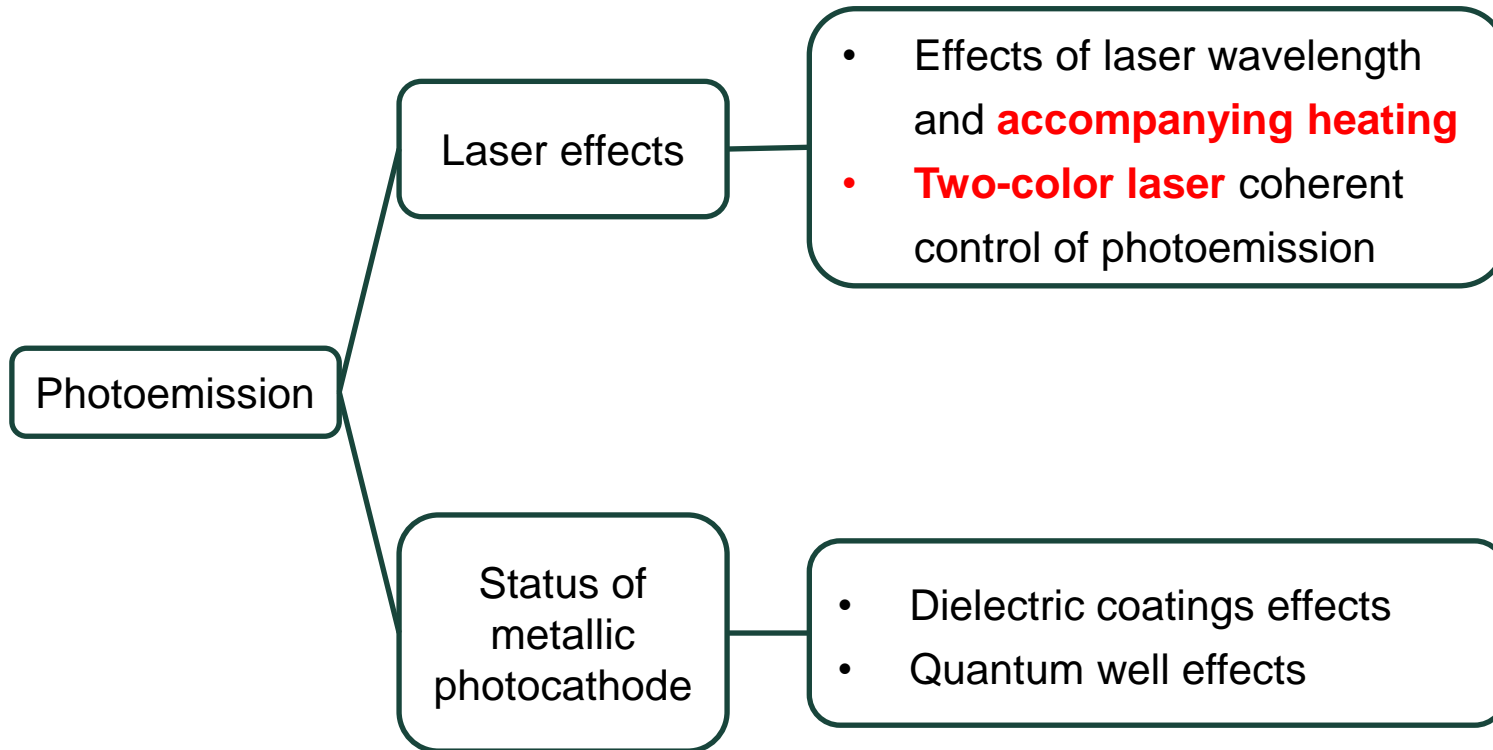
Resonant Tunneling Enhanced Field Emission



3.07 A/m²
105 A/m²

- Potential to produce **highly intense** and **highly collimated** electron beams

Summary



- Photo-/field/thermionic emission
- Integer of $W_0/\hbar\omega$
- Contribution from each pathway

- Enhanced field/photo- emission
- Plasmon-enhanced photoemission
- High-intensity and highly collimated electron beam

Q&A

Thank you!